



# A techno-economic investigation of conventional and innovative desiccant solutions based on moisture sorption analysis

Alessandro Giampieri<sup>\*</sup>, Yngrid Machado, Janie Ling-Chin, Anthony Paul Roskilly, Zhiwei Ma

Department of Engineering, Durham University, Durham, DH1 3LE, United Kingdom

## ARTICLE INFO

### Keywords:

liquid desiccant  
Surfactant and nanoparticles  
Ionic liquids  
Moisture absorption and desorption  
Techno-economic analysis

## ABSTRACT

Liquid desiccant technology is an energy-efficient substitute for technologies that are conventionally applied for temperature and humidity control; however, innovative desiccant solutions have not been extensively explored in terms of their performance and feasibility. This work aimed to investigate desiccant solutions with moisture sorption analysis technically and economically. Various conditions of temperature and humidity were tested in a climatic chamber and the moisture absorption and desorption capacity, thermo-chemical energy storage capacity, and cost of conventional and innovative desiccant solutions were assessed by experiment. Calcium chloride showed the highest moisture desorption capacity ( $0.3113 \text{ g}_{\text{H}_2\text{O}}/\text{g}_{\text{sol}}$  in the climatic chamber at  $50^\circ\text{C}$  and 25% RH) and the lowest cost, despite its low moisture absorption capacity. Ionic liquids show high moisture absorption capacity (as high as  $0.429 \text{ g}_{\text{H}_2\text{O}}/\text{g}_{\text{sol}}$  in the climatic chamber at  $25^\circ\text{C}$  and 90% RH) and could be used as additives (in which a maximum increase of 84.1% was observed for moisture absorption capacity due to the addition of ionic liquids), and thus, they are promising substitutes for conventional desiccant solutions. As solutions for better performance under various conditions were identified, the study will advance liquid desiccant technology.

## 1. Introduction

Liquid desiccant technology exploits the affinity to water molecules of hygroscopic solutions, which can be used for a variety of applications, such as moisture control and removal, industrial drying at low temperatures, *etc.* [1]. Lithium chloride (LiCl), calcium chloride ( $\text{CaCl}_2$ ) and other hygroscopic aqueous solutions of halide salts are common working fluids for these systems, despite of their drawbacks such as being corrosive and prone to crystallisation [2]. Moreover, aqueous LiCl solution is expensive whereas aqueous  $\text{CaCl}_2$  solution cannot give satisfactory dehumidification performance for deep dehumidification processes. Aqueous potassium formate ( $\text{HCO}_2\text{K}$ ) solutions have been studied as a less corrosive alternative to aqueous solutions of halide salts because of their low corrosivity, low potential for crystallisation and good dehumidification performance [3]. Mixtures of desiccant salts have also been studied to maintain optimal performance at a reduced cost [4–6]. To date, solutions with surfactants added, nanofluids and ionic liquids have been explored as innovative solutions for liquid desiccant application for higher performance, reduced corrosiveness, evitable crystallisation, and lower cost.

<sup>\*</sup> Corresponding author.

E-mail address: [alessandro.giampieri@durham.ac.uk](mailto:alessandro.giampieri@durham.ac.uk) (A. Giampieri).

## Nomenclature

<i>[BMIM][BF<sub>4</sub>]</i>	1-butyl-3-methylimidazolium tetrafluoroborate
<i>[DMIM][OAc]</i>	1,3-dimethylimidazolium acetate
<i>[EMIM][OAc]</i>	1-ethyl-3-methyl imidazolium acetate
<i>[EMIM][MeSO<sub>3</sub>]</i>	1-ethyl-3-methylimidazolium methanesulfonate
<i>[EMIM][BF<sub>4</sub>]</i>	1-ethyl-3-methylimidazolium tetrafluoroborate
<i>[Ch][DMPO<sub>4</sub>]</i>	2-hydroxy-N,N,N-trimethylethan-1-aminium dimethyl phosphate
<i>Al<sub>2</sub>O<sub>3</sub></i>	aluminium oxide
<i>CaCl<sub>2</sub></i>	calcium chloride
<i>CNT</i>	carbon nanotube
<i>CuO</i>	copper oxide
<i>IL</i>	ionic liquid
<i>Fe</i>	iron
<i>Fe<sub>2</sub>O<sub>3</sub></i>	iron oxide
<i>LiBr</i>	lithium bromide
<i>LiCl</i>	lithium chloride
<i>MWNT</i>	multi-walled carbon nanotube
<i>NP</i>	nanoparticle
<i>PVP</i>	polyvinylpyrrolidone
<i>HCO<sub>2</sub>K</i>	potassium formate
<i>SiO<sub>2</sub></i>	silicon dioxide
<i>[P<sub>4441</sub>][DMPO<sub>4</sub>]</i>	tributyl(methyl)phosphonium dimethyl phosphate

## Variables

<i>ω</i>	moisture content ( $g_{H_2O}/kg_{dry,air}$ )
<i>x</i>	mass fraction ( $g_{salt}/g_{sol}$ )
<i>MAC</i>	moisture absorption capacity ( $g_{H_2O}/g_{sol}$ )
<i>MDC</i>	moisture desorption capacity ( $g_{H_2O}/g_{sol}$ )
<i>C</i>	cost (£)
<i>M</i>	mass (g)
<i>T</i>	temperature (°C)
<i>RH</i>	relative humidity (%)

## Subscript

<i>eq</i>	equilibrium of the solution
<i>dry air</i>	air
<i>dil</i>	diluted solution
<i>conc</i>	concentrated solution
<i>sol</i>	solution
<i>sp</i>	specific
<i>THC</i>	temperature and humidity chamber
<i>H<sub>2</sub>O</i>	water

Nanofluids are engineered fluids that are obtained by suspending particles with sizes ranging 1–100 nm in water, oil, ethylene glycol, and other base fluids. Nanoparticles (NPs) used in nanofluids are carbon materials, metals, graphite, graphene, diamond, metal oxides, graphene oxide, etc. [7]. When NPs are added to desiccant solutions, this results in an increase in interactions and collisions between the NPs and the desiccant solution, which increases the solution's turbulence, fluctuations and heat and mass transfer [8]. In addition, nanofluids employing metal NPs (e.g., gold and silver) and metal oxides NPs (e.g., copper oxide (CuO), zinc oxide (ZnO), aluminium oxide (Al<sub>2</sub>O<sub>3</sub>), titanium oxide (TiO<sub>2</sub>), magnesium oxide (MgO), etc.) could enhance the sanitising property of conventional liquid desiccant solutions [9] due to their ability to inhibit the activity of fungi, viruses, and bacteria [10]. Ali et al. [11,12] found no significant effect on the performance when ultrafine particles of copper (Cu) were added to an aqueous CaCl<sub>2</sub> solution in a falling film dehumidification system. Kang et al. [13] observed increased mass transfer where the best performance was obtained for carbon nanotube (CNT) NPs (up to 2.48 times higher than the base fluid for a concentration of the NPs of 0.1% wt.) when iron (Fe) and CNT NPs (0.01–0.1% wt.) were added in a falling film dehumidification system using aqueous LiBr solution as the desiccant solution. Kim et al. [14] mixed silicon dioxide (SiO<sub>2</sub>) NPs (0.01–0.1% vol.) with an aqueous LiBr solution in a falling film dehumidifier by using ultrasonic disruption and magnetic stirring techniques. The surfactant 2E1H with a concentration of 150 ppm was added to the solution. Heat and mass transfer increased by 46.8% and 18% for 0.005% vol. SiO<sub>2</sub>. Langroudi et al. [15] reported a 12.23% and 13.22% increase in heat and mass transfer when gamma-phase aluminium oxide ( $\gamma$ -Al<sub>2</sub>O<sub>3</sub>) NPs (0.02% wt.) were added to an aqueous LiBr solution. The nanofluid was prepared by using ultrasonic disruption and magnetic stirring techniques. Wen et al. [16,17] observed an

increase in the dehumidification and regeneration rate of 25.9% and 24.7%, respectively, when multi-walled carbon nanotube (MNWT) (0.1% wt.) was tested in a falling film internally cooled dehumidifier and internally heated regenerator where surfactant polyvinylpyrrolidone (PVP-K30) (0.4% wt.) was added for stabilisation. Talal [18] simulated the increase in performance due to the addition of the NPs ( $\text{Al}_2\text{O}_3$ , Cu and  $\text{SiO}_2$ ) in counter and parallel flow falling film dehumidifiers, identifying an increase in the dehumidification performance due to the addition NPs that depends on the flow configuration of the dehumidification unit. Shoaib et al. [8] investigated the increase in performance due to the addition of CuO NPs (0.35% vol.) in a counter flow packed bed dehumidifier, showing increased mass transfer (average rate of  $4.5 \text{ g/m}^2\text{-sec}$ ). The nanofluid was prepared using an ultrasonic bath technique for 3 h. Zheng et al. [19] investigated the increase in performance due to the addition of  $\text{SiO}_2$  NPs (1% and 2% wt.) in a gas-liquid hollow fibre membrane dehumidifier, identifying an increase in the absorption performance that is proportional to the concentration of NPs in the nanofluid (up to 2.39 times of the base fluid for 2% wt. NP). In addition, the nucleation sites for crystal growth could be increased by adding NPs [20], which could be beneficial in absorption-based thermal batteries for thermo-chemical energy storage. Lin et al. [20] reported enhanced heat and cold storage density by 24.8% and 156%, respectively, when  $\text{SiO}_2$  NPs mixed with a LiCl crystallised slurry were tested.

The stability of nanofluids is a major problem for their application in liquid desiccant systems. The key requirements for the use of nanofluids are (i) to produce an even, stable and durable suspension, (ii) with a negligible agglomeration of particles and (iii) no chemical changes in the fluid [21]. The stability of the nanofluid could be enhanced by adding surfactants to it (in addition to the possibility of adding the surfactant to the stand-alone conventional desiccant solution) [22]. For application in “open” systems, the surfactant is required to be non-volatile, odourless and non-toxic. As reviewed by Wen and Lu [22], most of the surfactants added to the working fluids in absorption refrigeration or heat pump systems present small to high toxicity and odours and, as such, their use is not feasible in liquid desiccant systems. On the other hand, PVP-K30 is a water-soluble polymer, hygroscopic, characterised by good adhesive properties and stable pH, which represents a suitable candidate for the mixture with desiccant solutions [22]. When PVP-K30 was added to an aqueous LiCl solution for both the dehumidification and the regeneration process, Wen et al. [23,24] found that the increase in the concentration of the surfactant in the LiCl solution would reduce the contact angle on a stainless steel plate before levelling off. In a falling film internally cooled or heated system, their results showed that by adding PVP-K30 (which enlarged the wetting area whilst reducing the falling film thickness), dehumidification and regeneration rates would be increased by up to 22.7% and 26.3%, respectively. Hu et al. [25] added PVP-K30 to an aqueous LiBr solution for volatile organic compounds (VOCs) removal and found that the use of PVP-K30 would enhance both the solubility of hydrophobic VOCs in the desiccant solution as well as mass transfer at the solution interface.

Ionic liquids (ILs) were investigated as replacements for conventional desiccant solutions due to their solubility at ambient temperature (*i.e.* no problems of crystallisation), low or negligible corrosiveness and very low vapour pressure (*i.e.* very high dehumidification performance) [2]. In comparing the performances of 1-ethyl-3-methylimidazolium tetrafluoroborate ([EMIM][BF<sub>4</sub>]) (83.2% wt.) and aqueous LiBr solution (45% wt.) for a counter-flow dehumidifier, Luo et al. [26] found that the [EMIM][BF<sub>4</sub>] aqueous solution showed a lower dehumidification rate by about 13%. When the performances of 1-butyl-3-methylimidazolium tetrafluoroborate ([BMIM][BF<sub>4</sub>]) (85.5% wt.), 1,3-dimethylimidazolium acetate ([DMIM][OAc]) (81.3% wt.), aqueous LiCl (40.9% wt.), and LiBr solution (45% wt.) in a counter-flow dehumidifier were compared, Luo et al. [27] reported a similar dehumidification rate for the ILs and the conventional desiccant fluids where the best performance was shown by [DMIM][OAc] among the ILs. Qu et al. [28] calculated the thermo-physical properties useful for air-conditioning applications (such as the equilibrium vapour pressure, the specific heat capacity, the density and the dynamic viscosity) of 1-ethyl-3-methyl imidazolium acetate ([EMIM][OAc]). By analysing the dehumidification capacity of ILs (16 potential options in total), Watanabe et al. [29] found that tributyl (methyl)phosphonium dimethyl phosphate ([P<sub>4441</sub>][DMPO<sub>4</sub>]) (77% wt.) has the best performance because of its high dehumidification capacity, low corrosiveness and stability. Turnaoglu et al. [30] investigated a fibre bundle membrane dehumidifier using Sorbionic04, a mixture of 1-ethyl-3-methylimidazolium methanesulfonate ([EMIM][MeSO<sub>3</sub>]) with benzotriazole as corrosion inhibitor, as the desiccant solution, and the experimental results showed a good performance in terms of dehumidification effectiveness and compactness of the system. By investigating the dehumidification capacity of 7 potential ILs, Maekawa et al. [31] found that 2-hydroxy-N,N,N-trimethylethan-1-ammonium dimethyl phosphate ([Ch][DMPO<sub>4</sub>]) (80% wt.) would show the best performance due to its high dehumidification capacity, low corrosiveness, low cost and stability. By investigating the operation of a membrane-based heat and mass exchanger, Wang et al. [32] found reduced membrane contamination and increased durability of the dehumidifier when [EMIM][OAc] was used as the working fluid.

It is clear that several studies have investigated the use of innovative fluids in liquid desiccant systems — most of these studies focused on the performance of stand-alone solutions with limited studies comparing their performance with that of conventional desiccant solutions. In addition, most of the studies focused on the dehumidification process rather than the regeneration one (which could be beneficial for the investigation of the low-grade heat recovery capacity of desiccant solutions), showing the knowledge gap in the research on innovative fluids for liquid desiccant application. The literature review also showed that none of the studies has evaluated the cost and thermo-chemical energy storage capacity of using innovative fluids in liquid desiccant systems. As such, this study aims to investigate and compare the use of conventional and innovative desiccant solutions for the dehumidification and regeneration process by using a moisture sorption analysis, which is a technique that has been previously applied to adsorption processes in solid materials [33,34] instead of desiccant solutions. The objectives are (i) understanding the moisture absorption and desorption behaviour of conventional and innovative fluids with experiments; and (ii) assessing and comparing the feasibility of using innovative fluids from a techno-economic point of view. This study could be a base for developing liquid desiccant systems which requires the identification of the solutions for better performance under various conditions.

In this article, Section 2 presents the method applied to the study. Section 3 describes the procedure that was used to prepare the

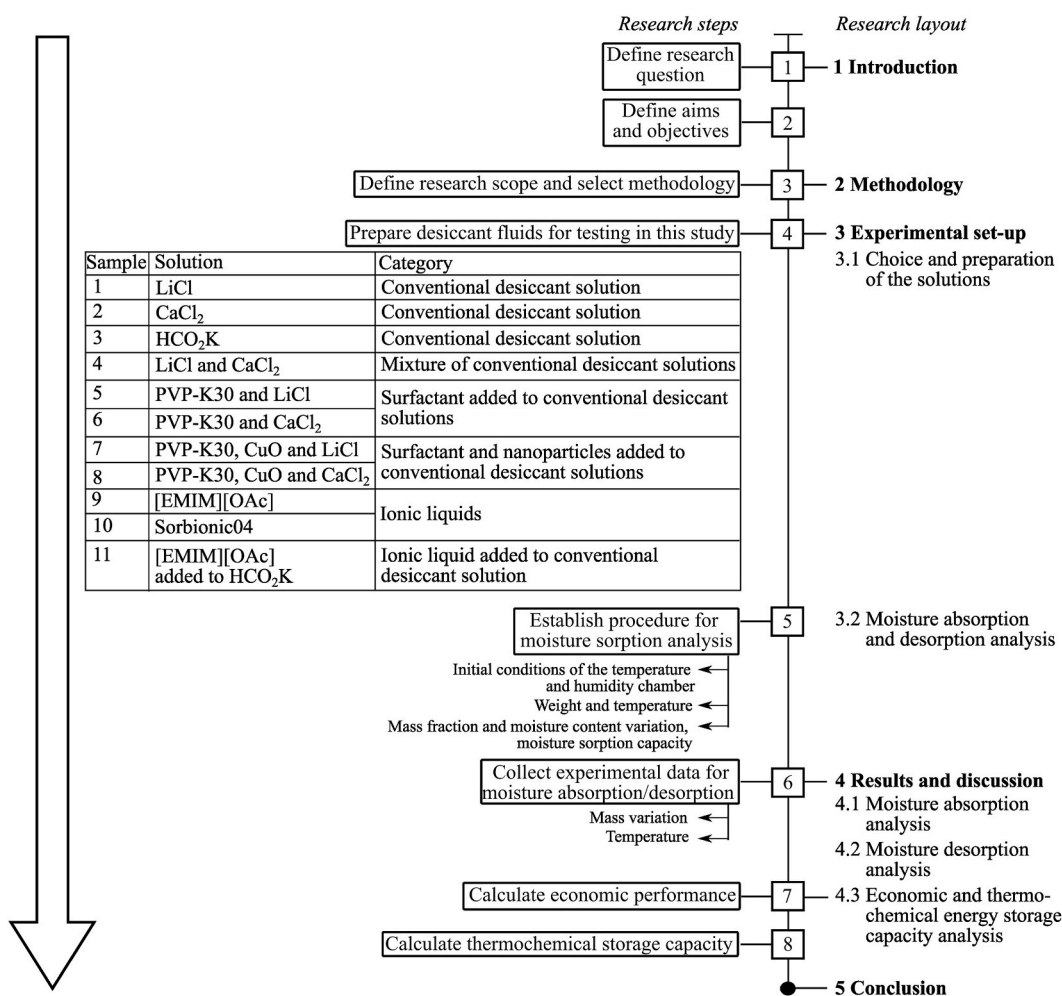


**Fig. 1.** Methodology applied for the techno-economic investigation based on moisture sorption analysis of conventional and innovative solutions used for liquid desiccant application.

**Table 1**

Characteristics of the desiccant salts, surfactants, NPs and ILs used in the study.

Component	Characteristics	Supplier	Justification of choice	Ref.
LiCl	Hygroscopic anhydrous salt (purity 99.3%) in the form of white crystalline powder	Leverton Lithium	Conventional desiccant solution	[35]
CaCl <sub>2</sub>	White, flaked, hygroscopic dihydrate salt with 77% wt. CaCl <sub>2</sub>	Tetra	Conventional desiccant solution	[36]
HCO <sub>2</sub> K	Soluble in water and very hygroscopic, purity 99% wt. (water content less than 2%)	Fisher Scientific	Conventional desiccant solution	[37]
PVP-K30	White to yellowish-white hygroscopic powder; 0.4% wt. PVP-K30 offers an optimal concentration in a desiccant solution [23,24]	Thermo Fisher Scientific	Non-volatile, odourless and non-toxic	[38]
CuO	Black coloured NPs with size of 30–40 nm and a specific surface area of 29 m <sup>2</sup> /g	Merck Life Science UK Limited	Antimicrobial; beneficial for application in highly occupied areas	[39, 40]
[EMIM][OAc]	Colourless to slightly yellow fluid, purity higher than 98% wt.	Proionic	High capacity for dehumidification [28], low corrosiveness [41], relatively low dynamic viscosity [42] and solubility at ambient temperature [43]	[44]
Sorbionic04	Slightly turbid yellow fluid	Proionic	High thermal stability and solubility at ambient temperature [43]	[44, 45]

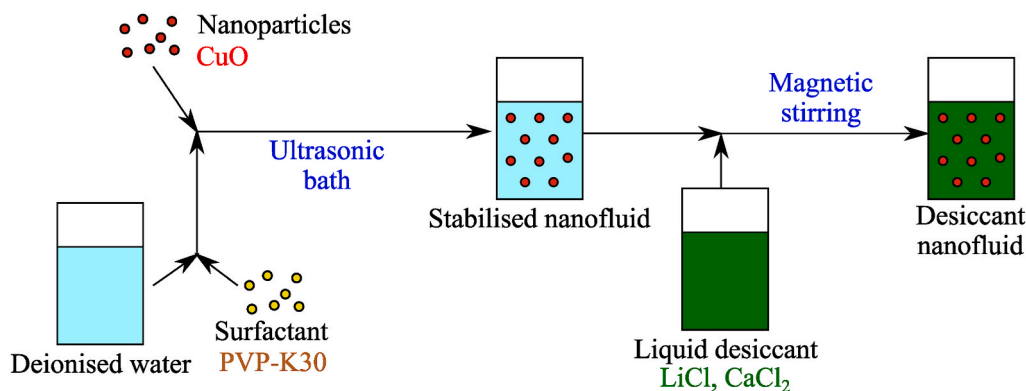


Fig. 2. Preparation of desiccant-based nanofluids with a two-step method, based on [14].

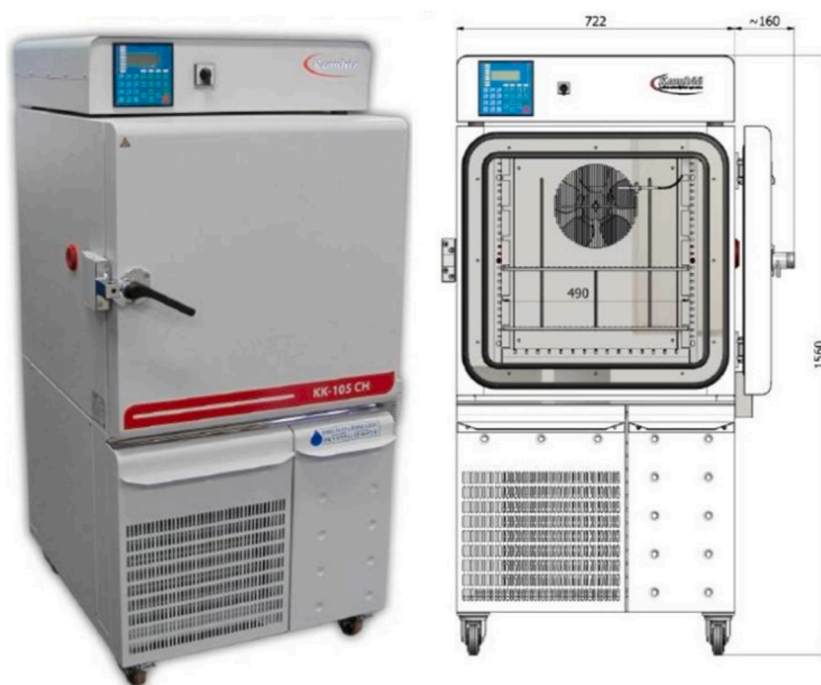


Fig. 3. The temperature and humidity chamber used for the moisture absorption and desorption analysis [46].

conventional and innovative desiccant solutions and the experimental setup for the moisture sorption analysis. Section 4 shows and discusses the results of the moisture absorption and desorption analysis, including the economic analysis of the use of conventional and innovative fluids and highlighting additional factors that must be considered when desiccant solutions are used for dehumidification and thermo-chemical energy storage in liquid desiccant systems.

## 2. Methodology

The methodology developed for the study is illustrated in Fig. 1, aiming to develop an approach that would enable the comparison of conventional and innovative desiccant solutions from a techno-economic point of view and help identify innovative desiccant solutions that could substitute for conventional desiccant solutions in the near future.

## 3. Experimental setup

### 3.1. Choice and preparation of the solutions

Table 1 summarises the characteristics of the desiccant salts (*i.e.*, LiCl, CaCl<sub>2</sub>, and HCO<sub>2</sub>K), surfactants (*i.e.*, PVP-K30), NPs (*i.e.*,

**Table 2**  
Experimental conditions set for the moisture absorption and desorption analysis.

	Condition	$T_{THC}$ (°C)	$RH_{THC}$ (%)	$\omega_{THC}$ (g <sub>H2O</sub> /kg <sub>dry air</sub> )	Number of experiments
Moisture absorption process	1	25	70	12.3	20
	2	18	95	13.9	49
	3	25	90	18	43
Moisture desorption process	1	40	35	16.3	10
	2	50	25	19.5	25
	3	45	35	21.3	24
	4	70	15	30.1	18
	5	90	15	72.1	12

**Table 3**  
Cost of desiccant salts, surfactants, NPs and/or ILs used in the study.

Material	C (£/kg)
LiCl	52.24
CaCl <sub>2</sub>	0.146
HCO <sub>2</sub> K	0.97
PVP-K30	8.82
CuO	123.96
[EMIM][OAc]	20.27
Sorbionic04	18.46

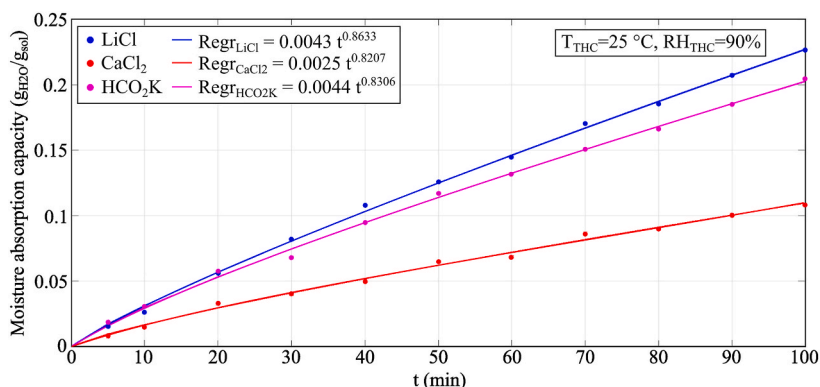


Fig. 4. Experimental results of the conventional desiccant fluids for moisture absorption analysis.

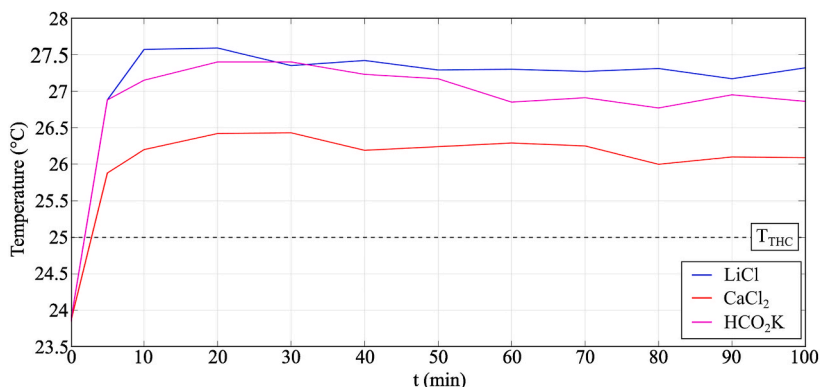


Fig. 5. Temperature variation of the samples during moisture absorption process in Condition 3 (T<sub>THC</sub> = 25 °C and RH<sub>THC</sub> = 90%).

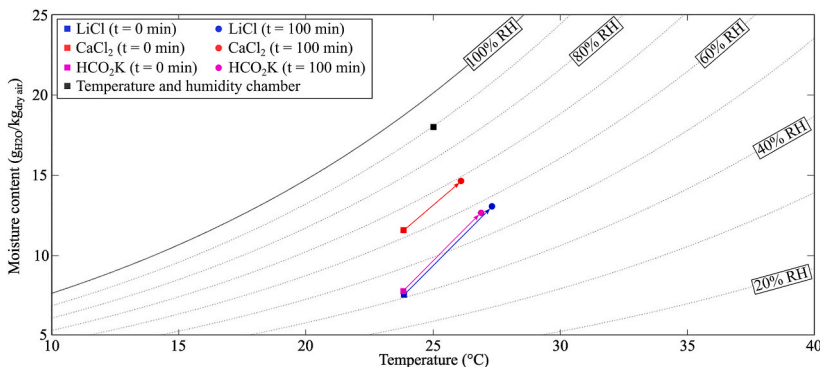


Fig. 6. Representation on a psychrometric chart of the moisture absorption process in Condition 3 ( $T_{THC} = 25\text{ }^{\circ}\text{C}$  and  $RH_{THC} = 90\%$ ).

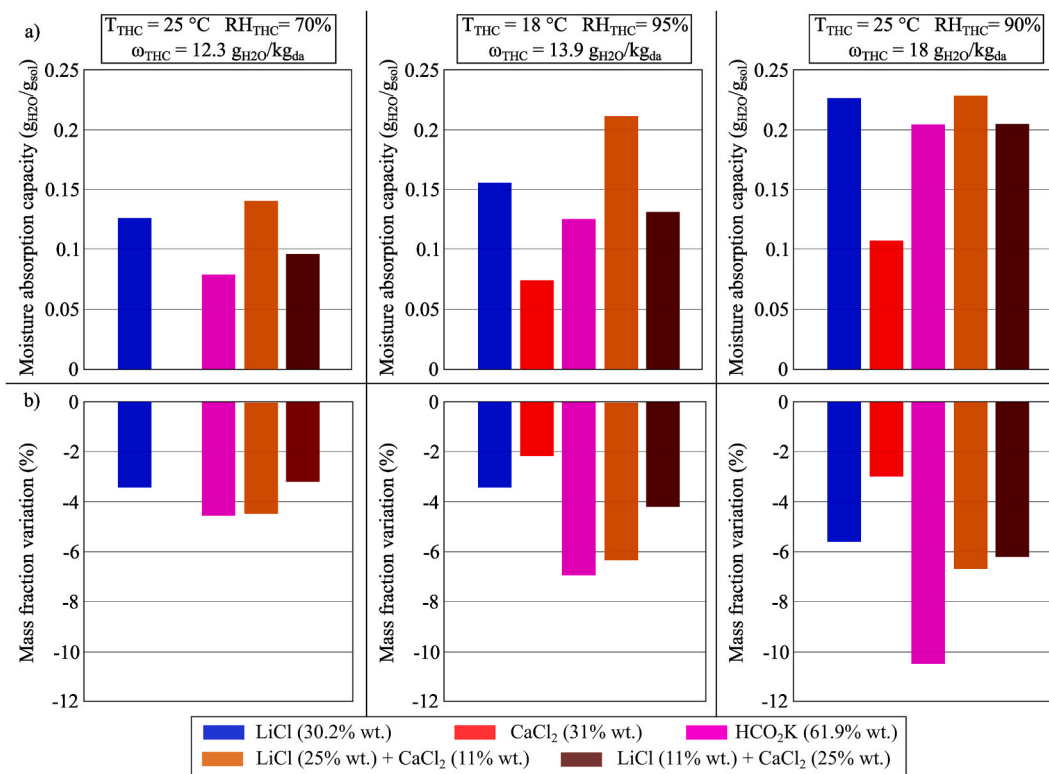
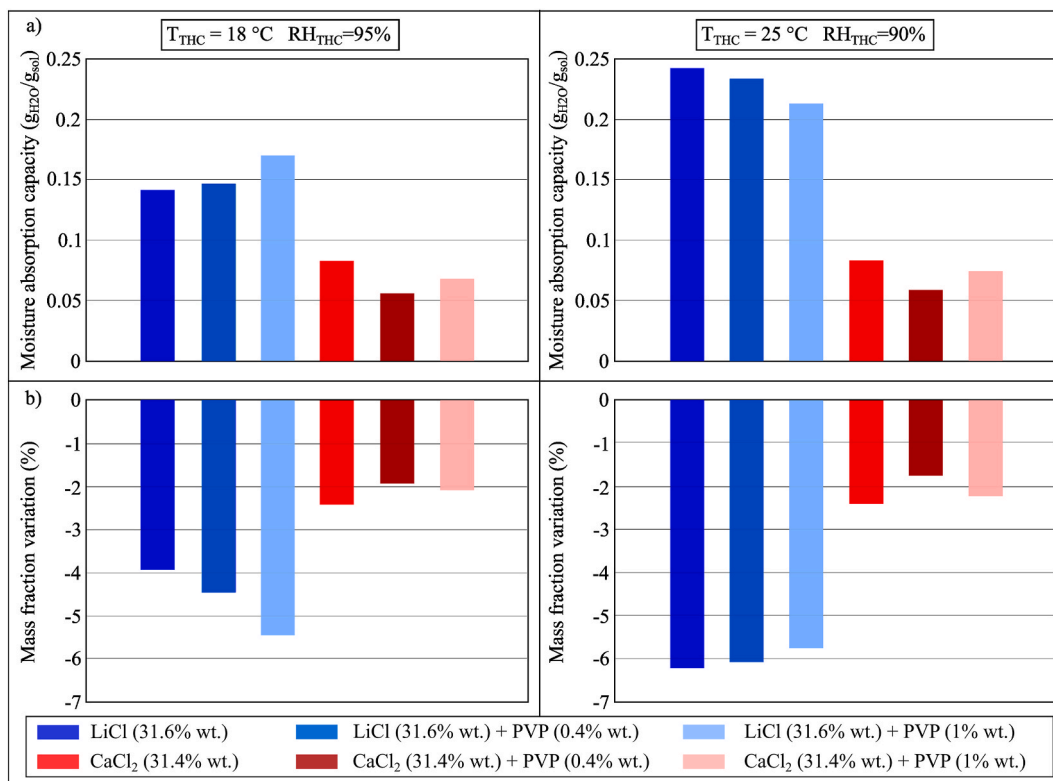


Fig. 7. (a) MAC and (b) mass fraction variation of conventional desiccant solutions and mixtures during the moisture absorption process after 100 min in Conditions 1 ( $T_{THC} = 25\text{ }^{\circ}\text{C}$ ,  $RH_{THC} = 70\%$ ), 2 ( $T_{THC} = 18\text{ }^{\circ}\text{C}$ ,  $RH_{THC} = 95\%$ ), and 3 ( $T_{THC} = 25\text{ }^{\circ}\text{C}$ ,  $RH_{THC} = 90\%$ ).

CuO) and ILs (i.e., [EMIM][OAc] and Sorbionic04) investigated in this study and why they were chosen. The mixtures of LiCl with  $\text{CaCl}_2$  were investigated, while the mixtures of LiCl and  $\text{CaCl}_2$  with  $\text{HCO}_2\text{K}$  were deselected as they would produce a chalky solution, which is not suitable for application in liquid desiccant air-conditioning systems.

Solutions required for experiments were prepared as described here. LiCl,  $\text{CaCl}_2$ ,  $\text{HCO}_2\text{K}$ , and PVP-K30 were solid crystals; as such, they were mixed with deionised water to achieve the percent by weight (% wt.) of each solution set for the experiments. Metal oxide-based nanofluids can be prepared in 2 ways, either the one-step or two-step method [7]: the one-step method involves a simultaneous synthesis and dispersion of metal oxide NPs in a base fluid; on the other hand, the two-step method involves the synthesis of metal oxide NPs first, followed by subsequent dispersion in the base fluid. The modified two-step method, as shown in Fig. 2, was selected for this study as it allowed the use of commercially available NPs i.e., CuO, to produce a satisfactory nanofluid for experiments. Ultrasonication was applied to intensify the dispersion of the CuO NPs into the base fluid and avoid their agglomeration [21]. A surfactant i.e., PVP-K30 (which alters the surface properties of the suspended particles and reduces the tendency of particles to stick together) was added to optimise the dispersion of the NPs in the solution [21]. Whilst the concentration of PVP-K30 in deionised water was selected



**Fig. 8.** (a) MAC and (b) mass fraction variation of conventional desiccant solutions and PVP-K30 during the moisture absorption process after 100 min in Conditions 2 ( $T_{\text{THC}} = 18 \text{ }^{\circ}\text{C}$ ,  $RH_{\text{THC}} = 95\%$ ) and 3 ( $T_{\text{THC}} = 25 \text{ }^{\circ}\text{C}$ ,  $RH_{\text{THC}} = 90\%$ ).

based on [23,24], 1% wt. PVP-K30 was also tested. For ILs, [EMIM][OAc] and Sorbionic04 manufactured by Proionic appeared in a liquid form. Therefore, pure and water-mixed [EMIM][OAc] and Sorbionic04 were tested in this study.

### 3.2. Moisture absorption and desorption analysis

The following procedure was applied for the moisture absorption and desorption analysis.

- 1) A temperature and humidity chamber (Manufacturer: Kambic, Model KK-105 CH with a temperature range of 5–180 °C and an RH range of 10–98%), as shown in Fig. 3, was used in this study to run experiments for moisture absorption and desorption analysis. The temperature and RH inside the chamber were fixed to meet the conditions set for the moisture absorption and desorption processes, as summarised in Table 2.
- 2) Samples of solutions were prepared where their temperatures were recorded. The weight of the samples was measured using a digital scale (Model Kern DS 150K1 with precision  $\pm 0.02$  g).
- 3) Variations in temperature due to the moisture absorption and desorption processes were determined using a K-type thermocouple linked to a PicoLog TC-08 thermocouple data logger [56].
- 4) Variations in mass fraction,  $x_{\text{sol}}$ , were then calculated. In addition, for conventional desiccant solutions, the variations in equilibrium moisture content,  $\omega_{\text{eq}}$ , of the solutions were calculated. The correlations for the equilibrium moisture content of LiCl and CaCl<sub>2</sub> were obtained from Ref. [53], while that of HCO<sub>2</sub>K was found in Ref. [54].
- 5) The moisture absorption capacity,  $MAC$  (g<sub>H2O</sub>/g<sub>sol</sub>), and the moisture desorption capacity,  $MDC$  (g<sub>H2O</sub>/g<sub>sol</sub>), were calculated using Eqs. (1) and (2) [57]:

$$MAC = \frac{M_f - M_i}{M_i} \quad (1)$$

$$MDC = \frac{M_i - M_f}{M_i} \quad (2)$$

where  $M_f$  and  $M_i$  represent the final and initial mass (g) of a sample after the moisture sorption process, respectively.

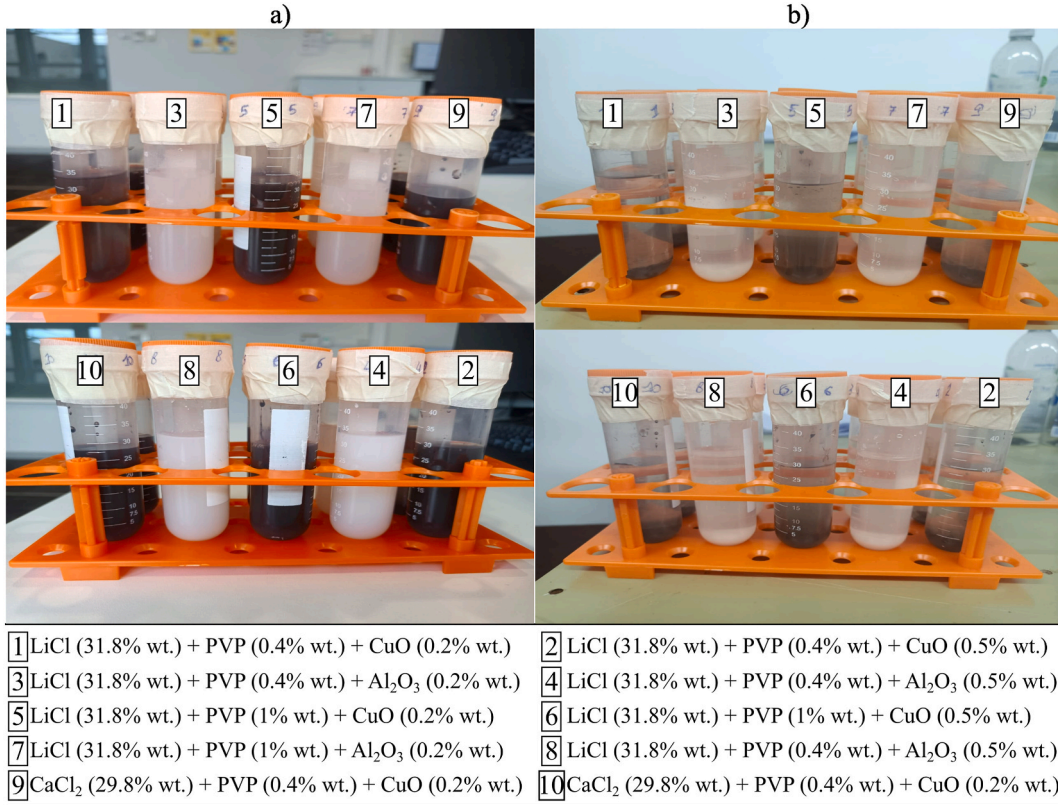


Fig. 9. Nanofluids prepared for the moisture absorption analysis. Photos were taken (a) immediately after preparation and (b) 6 h after preparation.

6) The economic performance of each solution was determined based on the costs of MAC and MDC,  $C_{MAC}$  ( $\text{g}_{\text{H}_2\text{O}}/\text{£}$ ) and  $C_{MDC}$  ( $\text{g}_{\text{H}_2\text{O}}/\text{£}$ ), using Eqs. (3) and (4):

$$C_{MAC} = \frac{M_f - M_i}{C_{M_i}} \quad (3)$$

$$C_{MDC} = \frac{M_i - M_f}{C_{M_i}} \quad (4)$$

where  $C_{M_i}$  is the cost (£) of the desiccant salts, surfactants, NPs and/or ILs used in preparing the solution, as shown in Table 3 [47–52].

7) The thermo-chemical energy storage potential of the desiccant solutions was compared based on the volumetric energy storage density,  $ESD$  ( $\text{kWh}/\text{m}^3$ ), as defined by Ref. [58] and reported in Eq. (5):

$$ESD = \rho_{dil} x_{dil} \left( \frac{1 - x_{conc}}{x_{conc}} - \frac{1 - x_{dil}}{x_{dil}} \right) (h_{fg}) \quad (5)$$

where  $\rho_{dil}$  is the density of the diluted desiccant solution ( $\text{kg}/\text{m}^3$ ),  $x_{dil}$  and  $x_{conc}$  are the mass fractions of the diluted and concentrated desiccant solutions ( $\text{kg}_{\text{salt}}/\text{kg}_{\text{sol}}$ ), respectively, and  $h_{fg}$  is the latent heat of evaporation of water ( $\text{kJ}/\text{kg}$ ). For the calculation, the density of aqueous solutions is obtained from literature: LiCl and  $\text{CaCl}_2$  [53];  $\text{HCO}_2\text{K}$  [54]; [EMIM][OAc] [28]; Sorbionic04 [45] (considering [EMIM][MeSO<sub>3</sub>] as fluid). The additive rule presented in Ref. [55] was applied to determine the density of mixtures.

## 4. Results and discussion

### 4.1. Moisture absorption analysis

#### 4.1.1. Conventional desiccant solutions

Fig. 4 illustrates the moisture absorption capacity of three aqueous solution samples of LiCl (30.2% wt.),  $\text{CaCl}_2$  (31% wt.) and  $\text{HCO}_2\text{K}$  (61.9% wt.) when the temperature and humidity chamber was set as 25 °C and 90% RH. The highest moisture absorption performance was shown by LiCl, followed by  $\text{HCO}_2\text{K}$  and  $\text{CaCl}_2$ . The moisture absorption process and the equilibrium moisture content

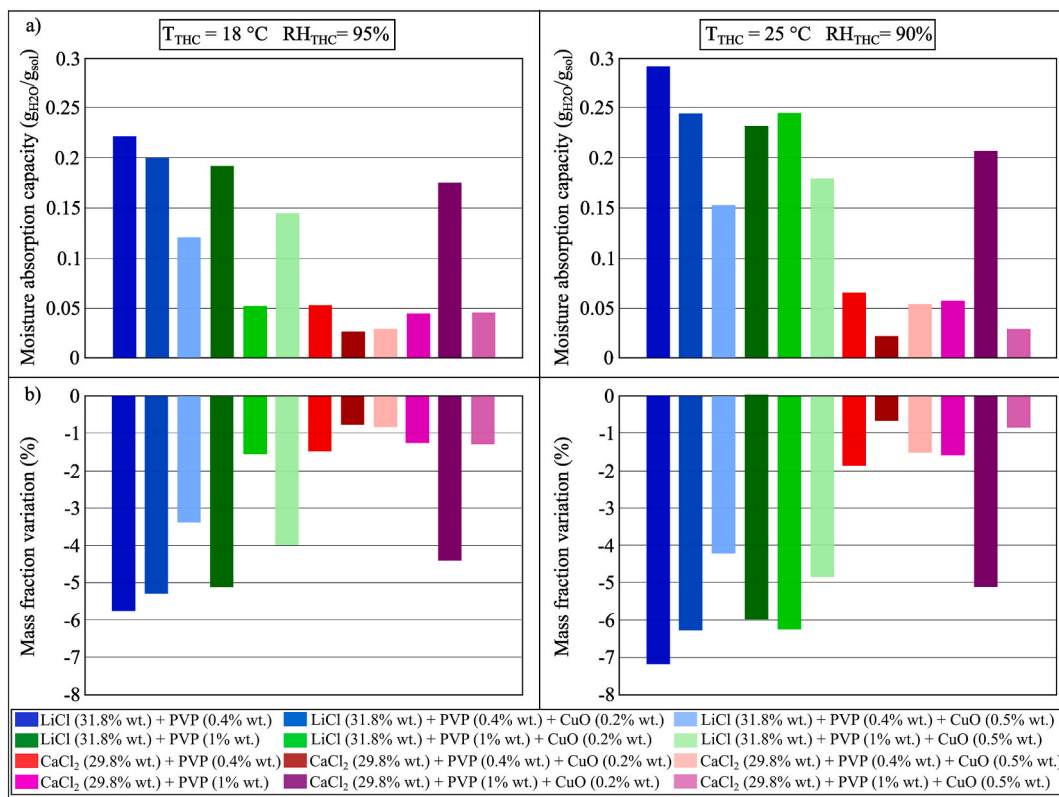


**Fig. 10.** (a) MAC and (b) mass fraction variation of conventional desiccant solutions, PVP-K30 and CuO during the moisture absorption process after 100 min in Conditions 2 ( $T_{\text{THC}} = 18^\circ\text{C}$ ,  $RH_{\text{THC}} = 95\%$ ), and 3 ( $T_{\text{THC}} = 25^\circ\text{C}$ ,  $RH_{\text{THC}} = 90\%$ ).

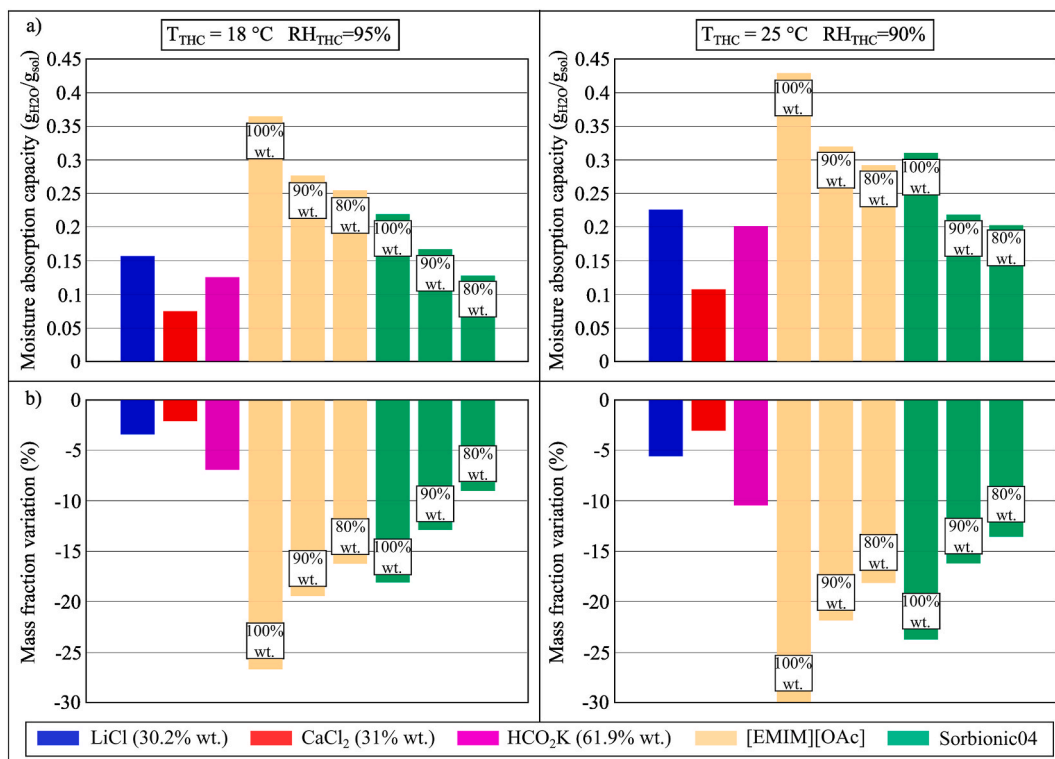
of a desiccant solution,  $\omega_{\text{eq}}$ , are in an inverse relationship: the lower the equilibrium moisture content, the higher the moisture absorption performance ( $\omega_{\text{LiCl}} = 7.59 \text{ g}_{\text{H}_2\text{O}}/\text{kg}_{\text{dry air}} < \omega_{\text{HCO}_2\text{K}} = 7.74 \text{ g}_{\text{H}_2\text{O}}/\text{kg}_{\text{dry air}} < \omega_{\text{CaCl}_2} = 10.83 \text{ g}_{\text{H}_2\text{O}}/\text{kg}_{\text{dry air}}$ ).

Fig. 5 shows the temperature variation of the samples during the experiment for the same condition of the temperature and humidity chamber, i.e.,  $25^\circ\text{C}$  and  $90\% \text{ RH}$ . When the desiccant solutions were placed in the temperature and humidity chamber, their initial temperatures were the same as the room temperature. At the start of the experiment, these solutions absorbed moisture from the surrounding air resulting in an increase in the temperature of each solution due to the latent heat of condensation. During the experiment, moisture absorbed by each solution from the air decreased over time because the solution was diluted by water absorption and consequently became less capable of absorbing moisture from the air, which resulted in a slight decrease in the temperature of the solution. As implied by the psychrometric chart in Fig. 6, the moisture absorption process would be driven by the difference between the equilibrium moisture content of the desiccant solution,  $\omega_{\text{eq}}$ , and the moisture content of the air in the temperature and humidity chamber,  $\omega_{\text{THC}}$ . During moisture absorption,  $\omega_{\text{eq}}$  increased as the desiccant solution absorbed moisture from the surrounding air and became diluted; the rate of moisture absorption by the desiccant solution reduced until, after sufficient time, absorption stopped as the solution reached a state of equilibrium. In this study, the largest difference between  $\omega_{\text{eq}}$  and  $\omega_{\text{THC}}$  was observed for the aqueous LiCl solution, which offered the best performing moisture absorption process compared to aqueous CaCl<sub>2</sub> and HCO<sub>2</sub>K solutions.

The moisture absorption performance of LiCl, CaCl<sub>2</sub>, HCO<sub>2</sub>K and mixtures of LiCl and CaCl<sub>2</sub> (for two different ratios) were investigated in three conditions of the temperature and relative humidity in the climatic chamber, and the results are illustrated in Fig. 7(a). The best moisture absorption performance was shown by the mixture of LiCl/CaCl<sub>2</sub> (25% wt./11% wt.), followed by LiCl (30.2% wt.), mixture of LiCl/CaCl<sub>2</sub> (11% wt./25% wt.), and HCO<sub>2</sub>K (61.9% wt.), in descending order. CaCl<sub>2</sub> (31% wt.) showed no moisture absorption in Condition 1 which has the lowest  $\omega_{\text{THC}}$  i.e.,  $12.3 \text{ g}_{\text{H}_2\text{O}}/\text{kg}_{\text{dry air}}$  compared to other conditions. As such, CaCl<sub>2</sub> should be deselected for deep dehumidification processes.

Fig. 7(b) shows the changes in the mass fraction of the investigated samples at the start and the end of the experiment. The magnitude is negative as the solution was diluted by the absorption process. In this study, HCO<sub>2</sub>K was the only solution working in the “water poor” mass fraction zone (i.e. the concentration of the water in the solution is lower than 50%). Desiccant samples operating with a water mass fraction lower than 50% would produce a larger mass fraction change between the beginning and the end of the moisture absorption process for the same amount of moisture absorbed. This affected the dehumidification capacity and thermochemical energy storage of the desiccant solution, as further described in Section 4.3.

Also implied in Fig. 7(a and b), an increase in  $\omega_{\text{THC}}$  would enhance the moisture absorption process performance. When CaCl<sub>2</sub> was used for moisture absorption, the sample was unable to absorb moisture from the air in Condition 1 (with the lowest  $\omega_{\text{THC}}$ ); it absorbed



**Fig. 11.** (a) MAC and (b) mass fraction variation of conventional desiccant solutions, [EMIM][OAc], and Sorbionic04 during the moisture absorption process after 100 min in Conditions 2 ( $T_{THC} = 18\text{ }^{\circ}\text{C}$ ,  $RH_{THC} = 95\%$ ) and 3 ( $T_{THC} = 25\text{ }^{\circ}\text{C}$ ,  $RH_{THC} = 90\%$ ).

moisture in Condition 2 ( $MAC_{CaCl_2} = 0.0743\text{ g}_{H_2O}/\text{g}_{sol}$ ) and its performance was further improved in Condition 3 ( $MAC_{CaCl_2} = 0.1079\text{ g}_{H_2O}/\text{g}_{sol}$ ). This trend was also shown by LiCl and HCO<sub>2</sub>K.

#### 4.1.2. Addition of surfactant

The addition of PVP-K30 would reduce the surface tension of the desiccant solution, which could be beneficial to the use in liquid desiccant systems by (i) creating a surface tension gradient at the interface between air and desiccant solution, which increases the mass transfer (this phenomenon is also known as the Marangoni effect [59,60]), and (ii) reducing the contact angle of the desiccant solution, resulting in an increase of the wetting ratio and a decrease of the film thickness. Desiccant systems with thin film could improve the moisture absorption process performance (*i.e.* dehumidification).

The moisture absorption performance of LiCl (31.6% wt.) and CaCl<sub>2</sub> (31.4% wt.) with and without PVP-K30 (0.4% wt. and 1% wt.) were compared, as shown in Fig. 8(a and b). However, these results indicated that the addition of PVP-K30 did not have a significant effect on the moisture absorption process; the type of base desiccant fluid would determine the moisture absorption capacity of the investigated sample. The moisture absorption capacity of LiCl samples was found higher than that of CaCl<sub>2</sub> samples. This could be due to the fact that the moisture absorption analysis is mainly ruled by the equilibrium vapour pressure and moisture content of the desiccant solution (as previously mentioned in Section 4.1.1) or to the inability of the testing method to capture the benefits of adding the surfactant to the desiccant.

#### 4.1.3. Addition of nanoparticles

The desiccant-based nanofluids prepared for the analysis, *i.e.*, PVP-K30 (0.4% or 1% wt.) with and without CuO NPs (0.2% or 0.5% wt.) added to LiCl or CaCl<sub>2</sub>, are shown in Fig. 9(a) after preparation and in Fig. 9(b) after 6 h. The produced samples indicated that the CuO-based nanofluids showed suspension instability. As illustrated in Fig. 10(a and b), the results showed that when CuO NPs were added to the mixture of LiCl or CaCl<sub>2</sub> and PVP-K30, the performance of the moisture absorption process for all samples, except for the mixture of CaCl<sub>2</sub> ( $x = 31.6\%$  wt.), PVP-K30 ( $x = 1\%$  wt.) and CuO ( $x = 0.2\%$  wt.), would reduce. The moisture absorption performance of the mixture of CaCl<sub>2</sub> ( $x = 31.6\%$  wt.), PVP-K30 ( $x = 1\%$  wt.) and CuO ( $x = 0.2\%$  wt.) is comparable with that of the LiCl samples. This shows that the increase in performance due to the addition of NPs is possible but the stability of the nanofluid may have a primary role in determining the moisture absorption capacity of a nanofluid. Similarly, a significant decrease in the moisture absorption performance of the samples using LiCl as the base desiccant salt could be attributable to the instability of the nanofluid.

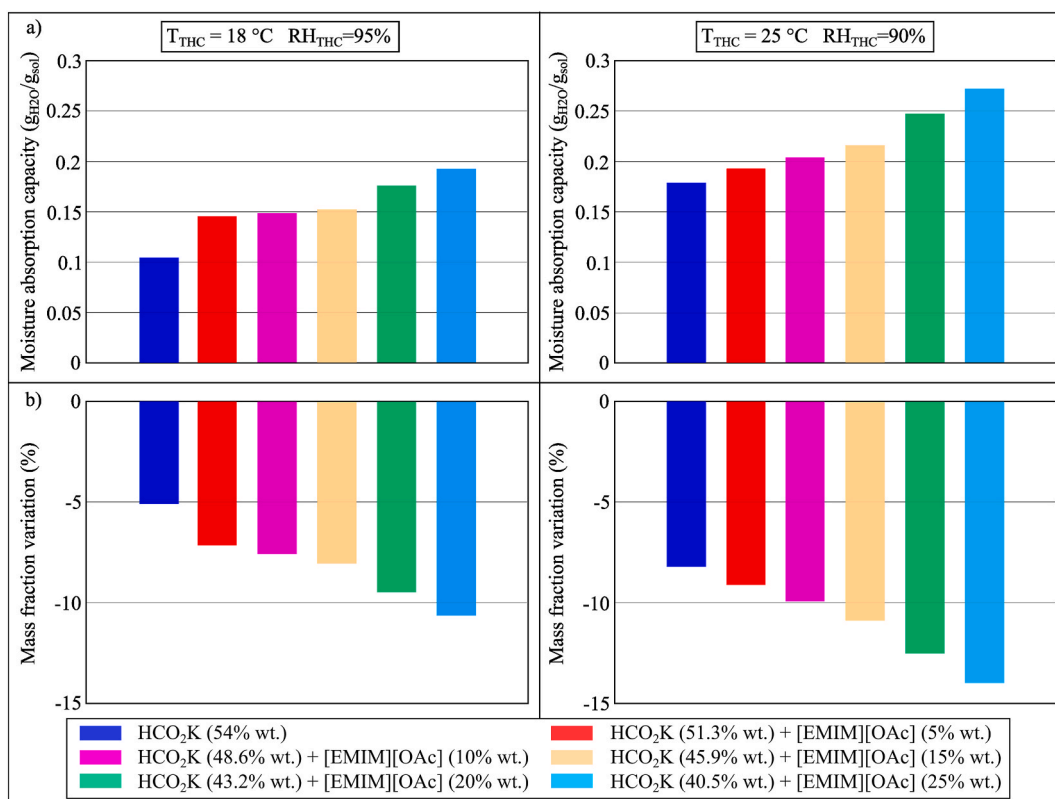


**Fig. 12.** (a) MAC and (b) mass fraction variation of HCO<sub>2</sub>K and the mixtures of HCO<sub>2</sub>K and [EMIM][OAc] during the moisture absorption process after 100 min in Conditions 2 ( $T_{THC} = 18\text{ }^{\circ}\text{C}$ ,  $RH_{THC} = 95\%$ ) and 3 ( $T_{THC} = 25\text{ }^{\circ}\text{C}$ ,  $RH_{THC} = 90\%$ ).

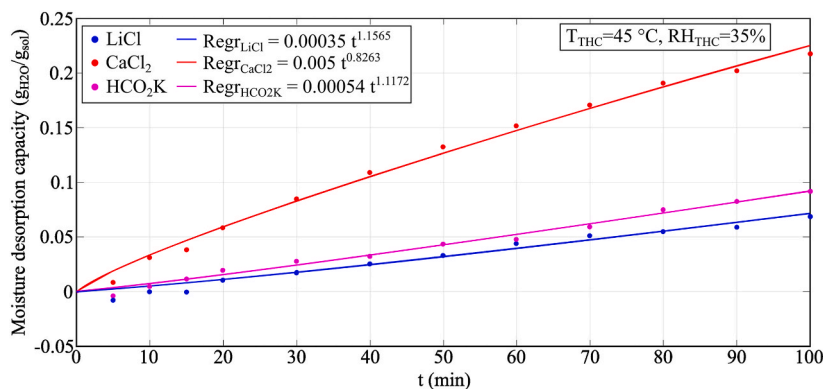


**Fig. 13.** Experimental results of LiCl, CaCl<sub>2</sub> and HCO<sub>2</sub>K during the moisture desorption analysis.

#### 4.1.4. Ionic liquids

The moisture absorption performance of two ILs, [EMIM][OAc] (80% wt., 90% wt., and 100% wt.) and Sorbionic04 (80% wt., 90% wt., and 100% wt.), were compared to LiCl (30.2% wt.), CaCl<sub>2</sub> (31% wt.) and HCO<sub>2</sub>K (61.9% wt.), as shown in Fig. 11(a and b). Whilst both [EMIM][OAc] and Sorbionic04 showed a better performance in the moisture absorption process compared to LiCl, CaCl<sub>2</sub> and HCO<sub>2</sub>K, [EMIM][OAc] (100% wt.) showed the highest moisture sorption capacity in the study, reaching 0.429  $g_{H_2O}/g_{sol}$  in the climatic chamber at 25  $^{\circ}\text{C}$  and 90% RH. Sorbionic04 showed a lower dehumidification performance than [EMIM][OAc]. In both Conditions 2 and 3 of the chamber, the moisture absorption capacity of Sorbionic04 (80% wt.) *i.e.*, 0.1265  $g_{H_2O}/g_{sol}$  and 0.204  $g_{H_2O}/g_{sol}$ , respectively, was similar to that of HCO<sub>2</sub>K (61.9% wt.) *i.e.*, 0.126  $g_{H_2O}/g_{sol}$  and 0.2038  $g_{H_2O}/g_{sol}$ , respectively, but lower than that of LiCl (30.2% wt.) *i.e.*, 0.156  $g_{H_2O}/g_{sol}$  and 0.226  $g_{H_2O}/g_{sol}$ .

In assessing the use of ILs as an additive, mixtures of LiCl, CaCl<sub>2</sub> and HCO<sub>2</sub>K with [EMIM][OAc] were assessed. The mixtures of LiCl and CaCl<sub>2</sub> with [EMIM][OAc] were deselected in this study as they produced a chalky solution. HCO<sub>2</sub>K and [EMIM][OAc] mixed well

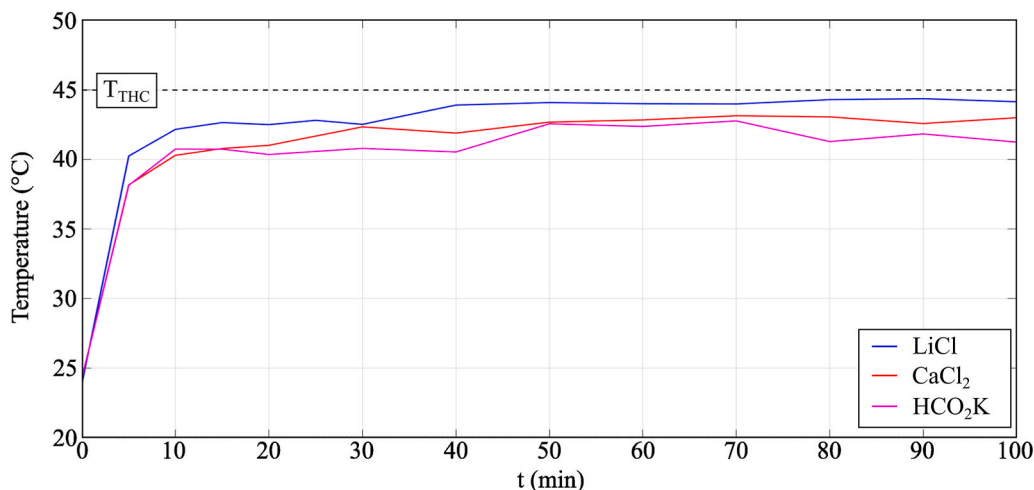


Fig. 14. Temperature variation of the samples during moisture desorption process in Condition 3 ( $T_{THC} = 45\text{ }^{\circ}\text{C}$  and  $RH_{THC} = 35\%$ ).

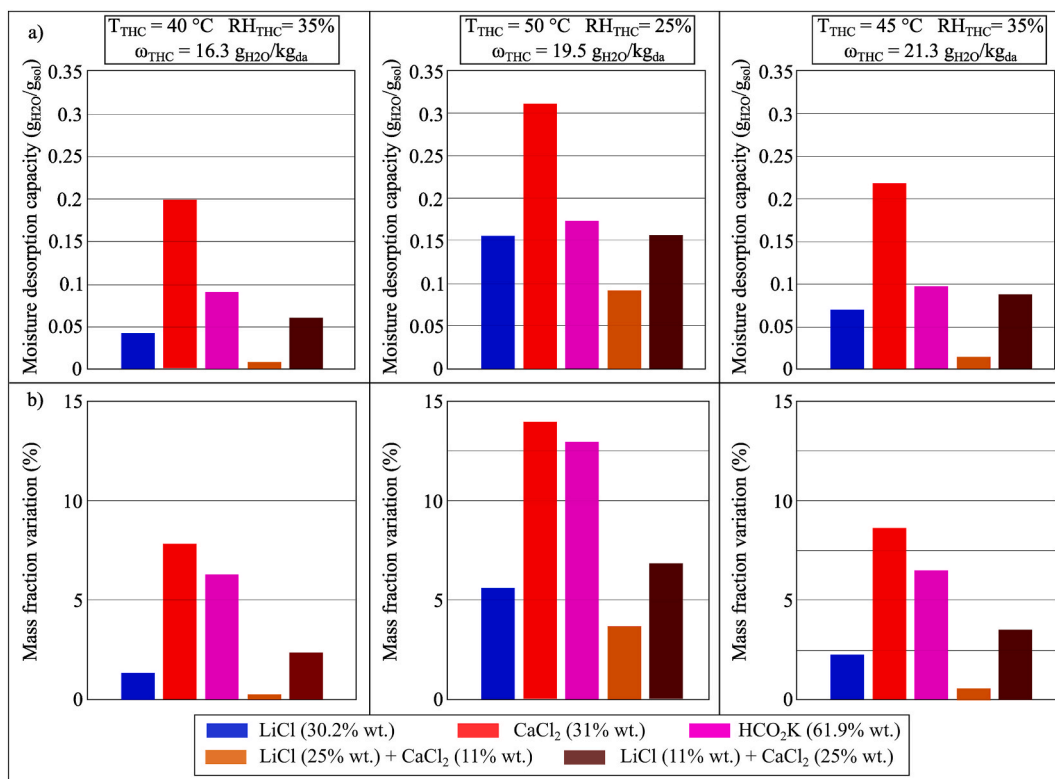


Fig. 15. (a) MDC and (b) mass fraction variation of conventional desiccant solutions and mixtures during the moisture desorption process after 100 min in Conditions 1 ( $T_{THC} = 40\text{ }^{\circ}\text{C}$ ,  $RH_{THC} = 35\%$ ), 2 ( $T_{THC} = 50\text{ }^{\circ}\text{C}$ ,  $RH_{THC} = 25\%$ ) and 3 ( $T_{THC} = 45\text{ }^{\circ}\text{C}$ ,  $RH_{THC} = 35\%$ ).

and the results in Conditions 2 ( $T = 18\text{ }^{\circ}\text{C}$ ,  $RH = 95\%$ ) and 3 ( $T = 25\text{ }^{\circ}\text{C}$ ,  $RH = 90\%$ ) were compared with that of aqueous HCO<sub>2</sub>K solution, as shown in Fig. 12(a and b). When the concentration of [EMIM][OAc] increased from 0% wt. (aqueous HCO<sub>2</sub>K solution) to 25% wt., its MAC would also increase significantly (0.1044 g<sub>H2O</sub>/g<sub>sol</sub> vs. 0.1922 g<sub>H2O</sub>/g<sub>sol</sub> and 0.1793 g<sub>H2O</sub>/g<sub>sol</sub> vs. 0.2706 g<sub>H2O</sub>/g<sub>sol</sub> in Conditions 2 and 3, respectively). This indicated the potential of adding [EMIM][OAc] to an aqueous HCO<sub>2</sub>K solution for deep dehumidification. Whilst HCO<sub>2</sub>K/[EMIM][OAc] would not present problems in terms of crystallisation, its corrosiveness should be further investigated.

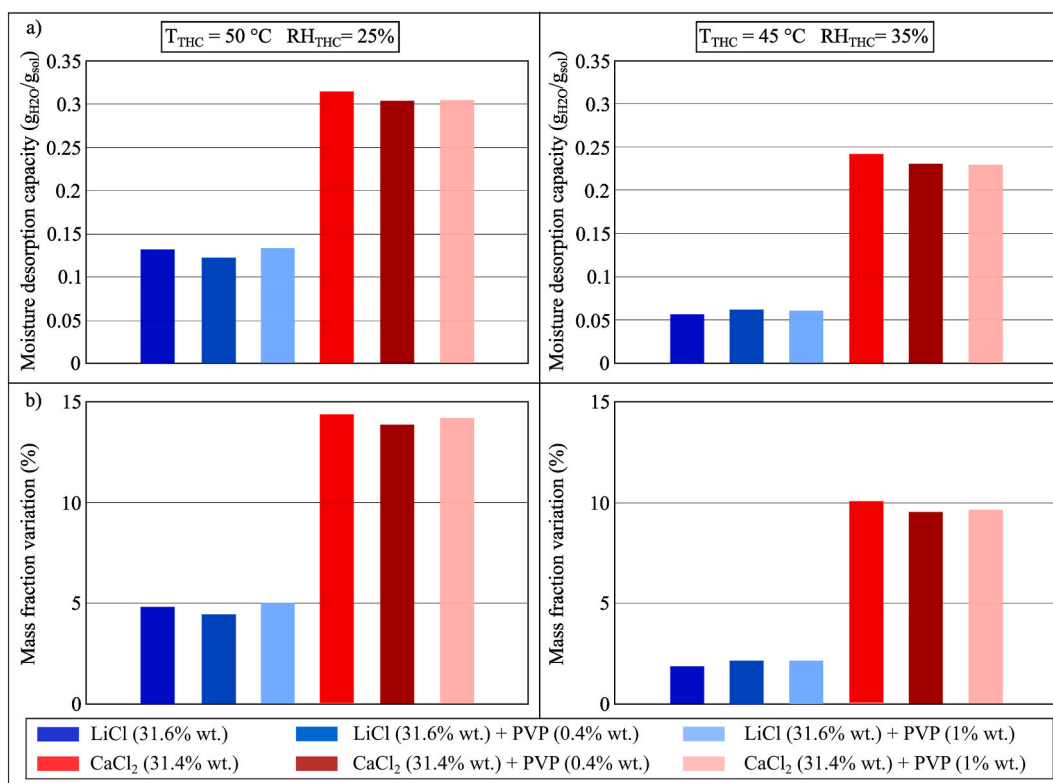


Fig. 16. (a) MDC and (b) mass fraction variation of conventional desiccant solutions and PVP-K30 during the moisture desorption process after 100 min in Conditions 2 ( $T_{THC} = 50\text{ }^{\circ}\text{C}$ ,  $RH_{THC} = 25\%$ ) and 3 ( $T_{THC} = 45\text{ }^{\circ}\text{C}$ ,  $RH_{THC} = 35\%$ ).

## 4.2. Moisture desorption analysis

### 4.2.1. Conventional desiccant solutions

Fig. 13 shows the moisture desorption capacity of LiCl (30.2% wt.), CaCl<sub>2</sub> (31% wt.) and HCO<sub>2</sub>K (61.9% wt.) for Condition 3 of the temperature and humidity chamber ( $T = 45\text{ }^{\circ}\text{C}$ ,  $RH = 35\%$ ). The highest moisture performance is shown by CaCl<sub>2</sub>, followed by HCO<sub>2</sub>K and LiCl. The moisture desorption process was affected directly by the equilibrium moisture content of the desiccant solution,  $\omega_{eq}$ : the higher the equilibrium moisture content, the higher the moisture absorption performance ( $\omega_{CaCl_2} = 10.83\text{ }g_{H_2O}/kg_{dry\ air} > \omega_{HCO_2K} = 7.74\text{ }g_{H_2O}/kg_{dry\ air} > \omega_{LiCl} = 7.59\text{ }g_{H_2O}/kg_{dry\ air}$ ). In this experiment, CaCl<sub>2</sub> showed a very high moisture desorption capacity (0.228  $g_{H_2O}/g_{sol}$ ) when the sample was 43.1  $^{\circ}\text{C}$ . This indicated the higher capacity of CaCl<sub>2</sub> to be regenerated by lower temperature heat sources, which could enhance the use of desiccant solutions to recover low-grade heat sources at about or slightly lower than 40  $^{\circ}\text{C}$ , such as hot water from compressed air units [61]. On the other hand, LiCl and HCO<sub>2</sub>K would require a temperature higher than 45  $^{\circ}\text{C}$  to provide a desorption process with good performance. Fig. 13 presented negative values of MDC for the LiCl and HCO<sub>2</sub>K samples in the first 15 min of the experiments (*i.e.*, moisture absorption rather than moisture desorption took place). As previously shown in Fig. 4, the desiccant solution samples would absorb moisture from the air straight away when experiments were started at room temperature. Unlike the moisture absorption process, the desiccant samples would need to reach a temperature higher than 40  $^{\circ}\text{C}$  at the start of the experiments to desorb moisture to the air in the climatic chamber.

The temperature variation profile for the moisture desorption process is shown in Fig. 14. The desorption of moisture from the desiccant solution to the air resulted in a decrease in the temperature of the samples compared to the temperature of the chamber caused by the latent heat of evaporation.

The moisture desorption performance of LiCl, CaCl<sub>2</sub>, HCO<sub>2</sub>K, and mixtures of LiCl and CaCl<sub>2</sub> (two different ratios) in three conditions of the temperature and humidity chamber were compared, as shown in Fig. 15(a and b). Compared to the moisture absorption process, the results showed that the moisture desorption process would be more affected by  $T_{THC}$  rather than  $\omega_{THC}$ . In Condition 2 ( $T_{THC} = 50\text{ }^{\circ}\text{C}$ ,  $RH_{THC} = 25\%$ ), aqueous CaCl<sub>2</sub> solution offered the highest MDC, 0.3113  $g_{H_2O}/g_{sol}$ . HCO<sub>2</sub>K (61.9% wt.) presented a slightly higher MDC than that of a mixture of LiCl and CaCl<sub>2</sub> (11% wt./25% wt.). However, similar to the findings reported in Section 4.1.1, with a concentration of water in the solution lower than 50%, HCO<sub>2</sub>K produced a larger mass fraction change between the beginning and the end of the moisture desorption process for the same amount of moisture desorbed, which would affect the capacity to store thermo-chemical energy of the desiccant solution as further discussed in Section 4.3.

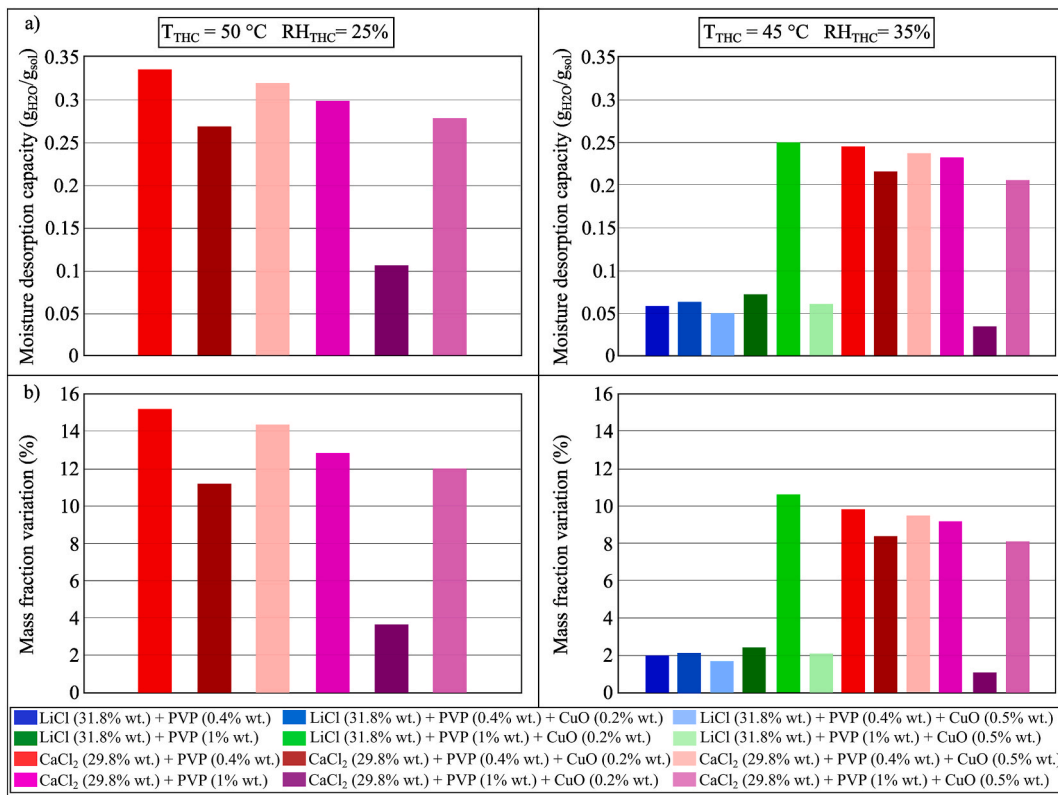


Fig. 17. (a) MDC and (b) mass fraction variation of conventional desiccant solutions, PVP-K30 and CuO during the moisture desorption process after 100 min in Conditions 2 (T<sub>THC</sub> = 50 °C, RH<sub>THC</sub> = 25%) and 2 (T<sub>THC</sub> = 45 °C, RH<sub>THC</sub> = 35%).

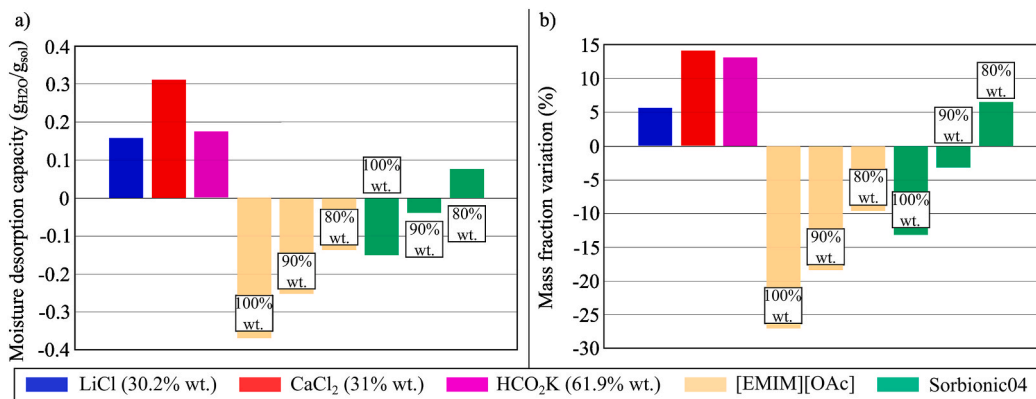
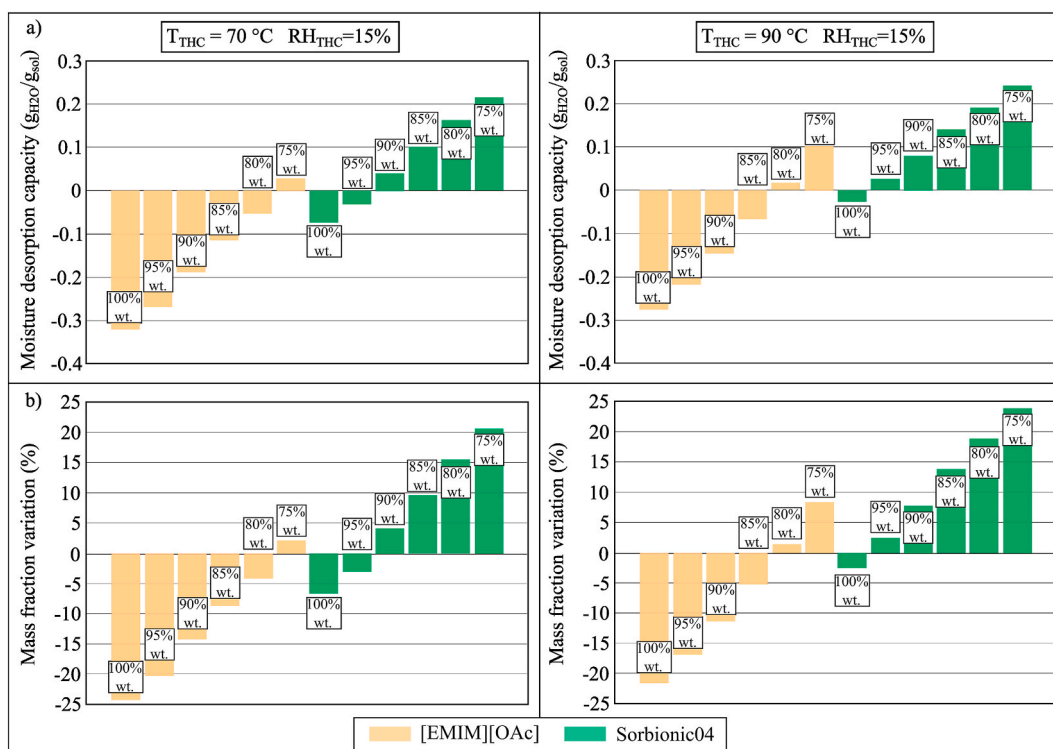


Fig. 18. (a) MDC and (b) mass fraction variation of unconventional desiccant fluids, [EMIM][OAc], and Sorbionic04 during the moisture desorption process after 100 min in Condition 2 (T<sub>THC</sub> = 50 °C, RH<sub>THC</sub> = 25%).

#### 4.2.2. Addition of surfactant

The moisture desorption performance of LiCl and CaCl<sub>2</sub> with and without PVP-K30 (0.4% and 1% wt.) were compared in Fig. 16(a and b). Similar to what was observed for the moisture absorption process, the addition of PVP-K30 would not have a significant effect on the performance of the desorption process. The type of base desiccant fluid would determine the moisture desorption capacity of the investigated sample, as evidenced by the higher moisture desorption capacity of CaCl<sub>2</sub> samples compared to LiCl samples, presumably because the moisture desorption analysis is mainly governed by the equilibrium vapour pressure and equilibrium moisture content of the desiccant solutions.



**Fig. 19.** (a) MDC and (b) mass fraction variation of [EMIM][OAc] and Sorbionic04 during the moisture desorption process after 100 min in Conditions 4 ( $T_{\text{THC}} = 70\text{ }^\circ\text{C}$ ,  $RH_{\text{THC}} = 15\%$ ) and 5 ( $T_{\text{THC}} = 90\text{ }^\circ\text{C}$ ,  $RH_{\text{THC}} = 15\%$ ).

#### 4.2.3. Addition of nanoparticles

The moisture desorption performance of LiCl and  $\text{CaCl}_2$  added with PVP-K30 (0.4% wt. and 1% wt.) with and without CuO (0.2% wt. and 0.5% wt.) were investigated, and the results are shown in Fig. 17(a and b). For most of the samples, a reduction in the moisture desorption performance was observed when CuO NPs were added. Compared to other  $\text{CaCl}_2$  samples, the mixture of  $\text{CaCl}_2$  (31.6% wt.), PVP-K30 (1% wt.) and CuO (0.2% wt.) (which offered a higher moisture absorption performance in Fig. 10) showed a significant drop in the moisture desorption performance. On the other hand, compared to other LiCl samples, the mixture of LiCl (29.8% wt.), PVP-K30 (1% wt.) and CuO (0.2% wt.) (which presented a lower moisture absorption performance in Fig. 10) showed a significant increase in the moisture desorption performance and became comparable to that of the  $\text{CaCl}_2$  samples. This implied that the addition of NPs could enhance the moisture desorption process but the stability of the produced nanofluid might determine its moisture desorption capacity.

#### 4.2.4. Ionic liquids

The moisture desorption performance of [EMIM][OAc] (80% wt., 90% wt., and 100% wt.) and Sorbionic04 (80% wt., 90% wt., and 100% wt.) were compared to that of LiCl (30.2% wt.),  $\text{CaCl}_2$  (31% wt.) and  $\text{HCO}_2\text{K}$  (61.9% wt.). The results in Fig. 18(a and b) indicated that when the temperature and humidity chamber was set to  $50\text{ }^\circ\text{C}$  and 25% RH, except for Sorbionic04 (80% wt.), all [EMIM][OAc] and Sorbionic04 samples would not desorb moisture but absorbed moisture from the air. Based on experimental results, only Sorbionic04 (80% wt.) showed the potential to be regenerated when its temperature ranged between 40 and  $44.4\text{ }^\circ\text{C}$ . To further evaluate the desorption capacity of [EMIM][OAc] and Sorbionic04 at higher temperatures, the moisture desorption tests were repeated at  $70\text{ }^\circ\text{C}$  and  $90\text{ }^\circ\text{C}$  while keeping the RH at 15%. The results are shown in Fig. 19(a and b), showing different behaviour during the moisture desorption of [EMIM][OAc] and Sorbionic04. For [EMIM][OAc], higher temperatures were required for regeneration. When the temperature and humidity chamber was  $70\text{ }^\circ\text{C}$  and 15% RH, only [EMIM][OAc] (75% wt.) was able to desorb moisture to the air but the performance was trivial ( $0.0276\text{ g}_{\text{H}_2\text{O}}/\text{g}_{\text{sol}}$ ) and the temperature of the sample could be as high as  $58\text{ }^\circ\text{C}$ . This indicated the potential of [EMIM][OAc] to perform moisture absorption (i.e. dehumidification) at relatively high temperatures, which could be beneficial for applications, such as industrial dryers [62] or automotive flash-off drying [63]. When the chamber was set to  $90\text{ }^\circ\text{C}$  and 15% RH, the moisture desorption performance of [EMIM][OAc] solution (75% wt.) increased to  $0.1\text{ g}_{\text{H}_2\text{O}}/\text{g}_{\text{sol}}$  and the temperature of the [EMIM][OAc] solution reached  $71.1\text{ }^\circ\text{C}$ . On the other hand, the moisture desorption performance of Sorbionic04 would be better, offering MDC of  $0.2154\text{ g}_{\text{H}_2\text{O}}/\text{g}_{\text{sol}}$  and  $0.2421\text{ g}_{\text{H}_2\text{O}}/\text{g}_{\text{sol}}$  in Conditions 4 and 5 of the temperature and humidity chamber ( $70\text{ }^\circ\text{C}$ , 15% RH and  $90\text{ }^\circ\text{C}$ , 15% RH, respectively), whereas the temperature of the sample reached  $57.4\text{ }^\circ\text{C}$  and  $66.3\text{ }^\circ\text{C}$ . In both Conditions 4 and 5, the temperature of Sorbionic04 samples was lower than that of [EMIM][OAc] samples.

The MDC and the mass fraction variation of the mixtures of  $\text{HCO}_2\text{K}$  and [EMIM][OAc] in Conditions 2 ( $50\text{ }^\circ\text{C}$ , 25% RH) and 4 ( $70\text{ }^\circ\text{C}$ , 15% RH) were compared with that of aqueous  $\text{HCO}_2\text{K}$  solution, as shown in Fig. 20(a and b). Unlike the findings shown in

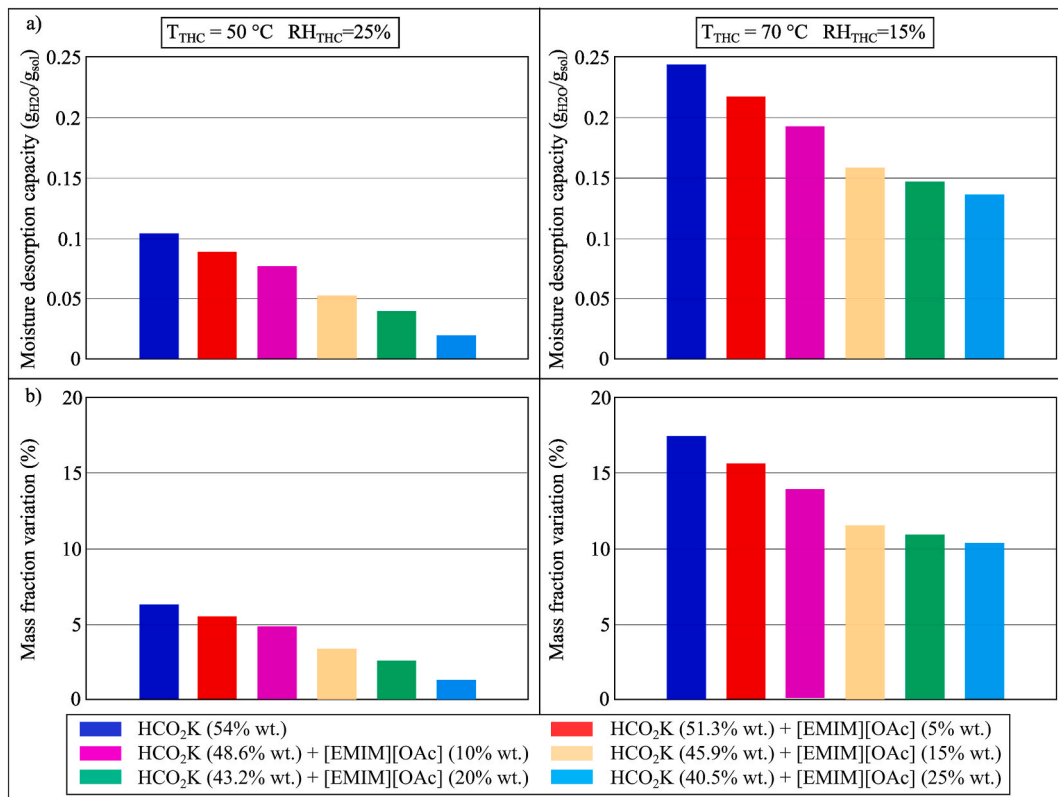


**Fig. 20.** (a) MDC and (b) mass fraction variation of the mixtures of HCO<sub>2</sub>K and [EMIM][OAc] during the moisture desorption process after 100 min in Conditions 2 ( $T_{THC} = 50$  °C,  $RH_{THC} = 25\%$ ) and 4 ( $T_{THC} = 70$  °C,  $RH_{THC} = 15\%$ ).

Figs. 12(a), Fig. 20(a) showed that the addition of [EMIM][OAc] to an aqueous HCO<sub>2</sub>K solution would reduce the MDC. When the concentration of [EMIM][OAc] increased from 0% wt. to 25% wt., the MDC of the solution in Conditions 2 and 4 of the temperature and humidity chamber would reduce from 0.104 g<sub>H2O</sub>/g<sub>sol</sub> to 0.0198 g<sub>H2O</sub>/g<sub>sol</sub> and from 0.244 g<sub>H2O</sub>/g<sub>sol</sub> to 0.136 g<sub>H2O</sub>/g<sub>sol</sub>, respectively. This implied the need for a higher temperature to effectively desorb the moisture from the desiccant solution when [EMIM][OAc] was added to the aqueous HCO<sub>2</sub>K solution.

#### 4.3. Economic and thermo-chemical energy storage capacity analysis

The trade-off between the performance of the moisture sorption process and the cost of the desiccant solution was evaluated using  $C_{MAC}$  and  $C_{MDC}$  defined in Section 3. The higher these values, the better the performance from a cost perspective. Fig. 21 presents the results of the analysis for the moisture absorption and desorption processes in two conditions of the temperature and humidity chamber ( $T_{THC} = 25$  °C,  $RH_{THC} = 90\%$ ; and  $T_{THC} = 50$  °C,  $RH_{THC} = 25\%$ , respectively) for some selected samples of each of the analyzed categories of conventional and innovative desiccant solutions.

The low cost of CaCl<sub>2</sub> strongly affects the economic performance of both the moisture absorption and desorption processes, ensuring a higher performance from a techno-economic point of view. However, it is worth mentioning that CaCl<sub>2</sub> would not be able to absorb moisture from the air if  $\omega_{air}$  is low, for example, when the temperature and humidity chamber is 25 °C and 70% RH as shown in Fig. 7. On the contrary, the high cost of LiCl limits its feasibility for moisture sorption from an economic point of view. Compared to LiCl, HCO<sub>2</sub>K is preferable as its cost is significantly lower whilst its moisture absorption capacity is similar to that of LiCl, which results in higher  $C_{MAC}$  and  $C_{MDC}$  (1797.7 g<sub>H2O</sub>/£ and 1498.3 g<sub>H2O</sub>/£ for HCO<sub>2</sub>K vs. 77.2 g<sub>H2O</sub>/£ and 51.9 g<sub>H2O</sub>/£ for LiCl, respectively). Mixtures of LiCl and CaCl<sub>2</sub> show the potential to increase economic performance. For instance,  $C_{MAC}$  and  $C_{MDC}$  of LiCl/CaCl<sub>2</sub> (11% wt./25% wt.) mixture are more than double that of LiCl. However, the lower moisture absorption capacity of the mixture compared to the stand-alone LiCl desiccant should be considered. When the mass fraction of LiCl increases, as in the mixture of LiCl (25% wt.) and CaCl<sub>2</sub> (11% wt.), the economic benefits of using mixtures are reduced.

The high potential of using [EMIM][OAc] in liquid desiccant systems, in particular for deep dehumidification processes, is justified by its high moisture absorption capacity and higher  $C_{MAC}$  compared to LiCl (90.03 g<sub>H2O</sub>/£ vs. 77.2 g<sub>H2O</sub>/£). However, the feasibility of using this IL for low-grade heat recovery is affected by the higher temperature required for the moisture desorption process. On the other hand, Sorbionic04 shows similar performance as LiCl for the moisture absorption process and lower performance for the moisture desorption process. This implies that Sorbionic04 could be used as a replacement for LiCl in liquid desiccant systems with the

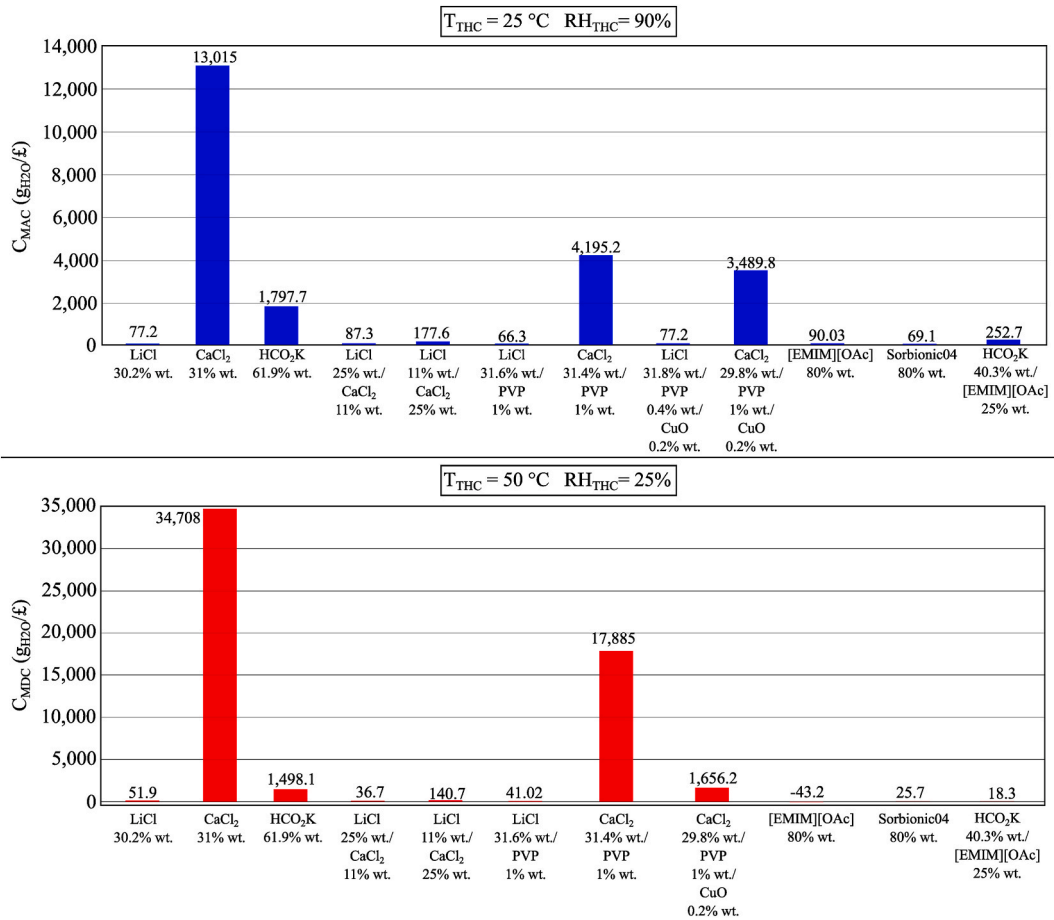


Fig. 21. Trade-off between the moisture sorption process performance and the cost of the desiccant solution.

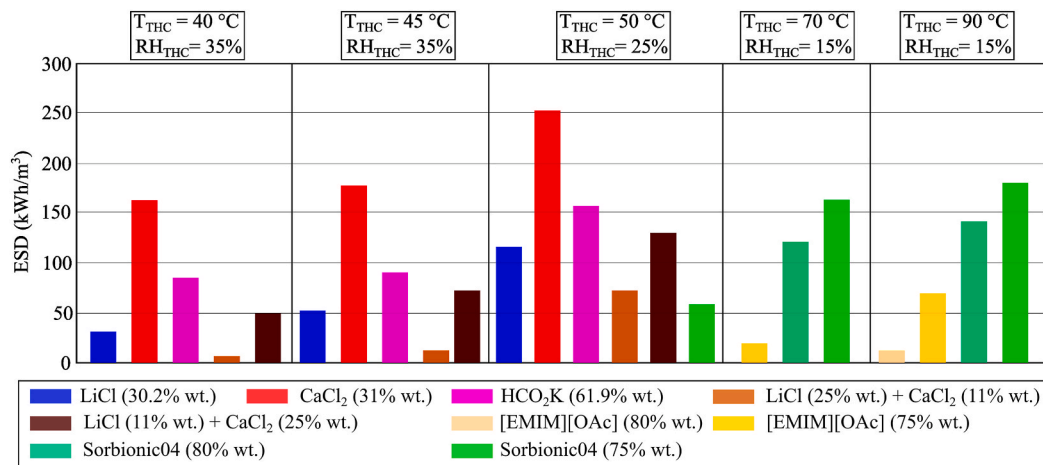


Fig. 22. Volumetric energy density of desiccant fluids based on moisture desorption analysis.

advantages of not producing crystals and being non-corrosive at the expense of requiring a heat source of a slightly higher temperature for efficient regeneration of the desiccant solution. The addition of PVP-K30 to the desiccant salt would not have a significant effect on the moisture sorption process performance, while the cost of the surfactant would have a limited impact on the economic performance of the moisture sorption process. The high cost of CuO NPs (123.96 £/kg) would reduce the economic performance despite its small

concentration.

When heat is supplied to a desiccant solution for regeneration (*i.e.*, moisture desorption), it increases the concentration of the desiccant solution, which can then be used for dehumidification (*i.e.*, moisture absorption) without a further supply of thermal energy. In this regard, the concentrated desiccant solution stores thermal energy in the form of thermo-chemical energy/absorption potential. As such, a larger concentration glide is required for storing a significant amount of thermo-chemical energy in the liquid desiccant solution. The effect of temperature and humidity on the volumetric energy storage density, *ESD*, was investigated for some selected desiccant samples based on the results of the moisture desorption analysis. As shown in Fig. 22, the *ESD* of the  $\text{CaCl}_2$  solution could reach  $252.6 \text{ kWh/m}^3$  when the temperature and humidity chamber was  $50^\circ\text{C}$  and 25% RH. This value indicated the high potential of  $\text{CaCl}_2$  for storing energy in the form of thermo-chemical energy compared to water (*ESD* of  $69.4 \text{ kWh/m}^3$  for a  $\Delta T$  of  $60^\circ\text{C}$  stored as sensible heat), underground materials, such as rock, dry and wet soil (*ESD* of  $30 \text{ kWh/m}^3$  for a  $\Delta T$  of  $50^\circ\text{C}$  stored as sensible heat), organic materials (*ESD* of  $27.8\text{--}69.4 \text{ kWh/m}^3$  stored as latent heat) and inorganic materials (*ESD* of  $41.7\text{--}119.4 \text{ kWh/m}^3$  stored as latent heat) [64]. In real operating liquid desiccant systems, low-flow technology is required to achieve a large concentration variation between the concentrated and the diluted solution [65]. Conventional technology usually involves high flow rates, which are required to limit the increase/decrease in the temperature of the desiccant solution while absorbing/desorbing moisture from/to the air. On the other hand, these internally cooled/heated systems use a lower solution flow rate, which allows achieving a larger difference in the solution concentration and, as such, storing higher thermo-chemical energy.

The results shown in Fig. 22 were estimated for the charging process of the thermo-chemical energy storage (*i.e.* moisture desorption). However, desiccant solutions capable of achieving a larger variation in concentration for the discharging process of the thermo-chemical energy storage would also be favoured for application in liquid desiccant systems since a lower concentrated solution (*i.e.*, higher  $\omega_{\text{eq}}$ ) would have a higher performance during regeneration (*i.e.*, moisture desorption), as shown by  $\text{HCO}_2\text{K}$  in Section 4.1.1. Similar to  $\text{HCO}_2\text{K}$ , [EMIM][OAc] and Sorbionic04 could also work if the concentration of water in the solution was lower than 50%. This would allow achieving a larger mass fraction variation between the beginning and the end of the moisture absorption process for the same amount of moisture absorbed, resulting in a diluted solution with higher moisture desorption capacity.

## 5. Conclusion

This study presented an experimental and feasibility investigation of desiccant solutions (either conventional or innovative) based on moisture sorption and techno-economic analyses to enhance the current understanding of moisture absorption and desorption behaviour and assess the feasibility of using innovative fluids.  $\text{CaCl}_2$  showed low moisture absorption performance but high moisture desorption capacity (up to  $0.3113 \text{ g}_{\text{H}_2\text{O}}/\text{g}_{\text{sol}}$  in the climatic chamber at  $50^\circ\text{C}$  and 25% RH, implying higher potential for low-grade heat recovery) and thermo-chemical energy storage capacity for charging ( $252.6 \text{ kWh/m}^3$  under the same climatic chamber condition). Ionic liquids were proved as feasible replacements for conventional desiccant solutions with larger moisture absorption capacity, such as  $\text{LiCl}$  and  $\text{HCO}_2\text{K}$ , due to their ability to provide high moisture absorption at relatively high temperatures, although these solutions showed a lower capacity to recover low-grade heat sources. A maximum moisture absorption capacity of  $0.429 \text{ g}_{\text{H}_2\text{O}}/\text{g}_{\text{sol}}$  was achieved for pure [EMIM][OAc] in the climatic chamber at  $25^\circ\text{C}$  and 90% RH. Ionic liquids could be used as additives to increase the performance of conventional desiccant solutions without having a significant effect on cost. The addition of PVP-K30 and  $\text{CuO}$  nanoparticles showed limited or no effect on the performance of the moisture absorption or desorption process. The high cost of  $\text{CuO}$  nanoparticles could limit the feasibility of nanofluids in liquid desiccant systems. The current research offers insights into what desiccant solutions could have the best performance and lowest cost under various conditions. Both kinetics and sorption rates have not been investigated in this study, neither has the use of all innovative solutions been trialled in real operating liquid desiccant systems, which present limitations of this study. As ionic liquids appeared more promising as shown by the results gained in this study, future research should investigate kinetics, sorption rates, and testing of the use of ionic liquids, both stand-alone and as additives, in real operating liquid desiccant systems.

## Author contribution statement

Alessandro Giampieri: Conceived and designed the experiments; Performed the experiments; Analyzed and interpreted the data; Contributed reagents, materials, analysis tools or data; Wrote the paper.

Yngrid Machado: Performed the experiments; Analyzed and interpreted the data.

Janie Ling-Chin: Analyzed and interpreted the data; Contributed reagents, materials, analysis tools or data; Wrote the paper.

Anthony Paul Roskilly: Contributed reagents, materials, analysis tools or data; Wrote the paper.

Zhiwei Ma: Conceived and designed the experiments; Wrote the paper.

## Data availability statement

Data will be made available on request.

## Declaration of competing interest

The authors declare that they have no known competing financial interests or personal relationships that could have appeared to influence the work reported in this paper.

## Acknowledgments

This research was funded by the Engineering and Physical Science Research Council (EPSRC) of the United Kingdom for a project entitled, "Decarbonisation of Low Temperature Process Heat Industry, DELTA PHI" (EP/T022981/1).

## References

- [1] A. Giampieri, et al., Liquid desiccant dehumidification and regeneration process: advancing correlations for moisture and enthalpy effectiveness, *Appl. Energy* 314 (2022), 118962.
- [2] A. Giampieri, et al., Thermodynamics and economics of liquid desiccants for heating, ventilation and air-conditioning—An overview, *Appl. Energy* 220 (2018) 455–479.
- [3] T. Wen, et al., Comparative study on the liquid desiccant dehumidification performance of lithium chloride and potassium formate, *Renew. Energy* 167 (2021) 841–852.
- [4] L. Xiu-Wei, et al., *Research on ratio selection of a mixed liquid desiccant: mixed LiCl–CaCl<sub>2</sub> solution*, *Sol. Energy* 82 (12) (2008) 1161–1171.
- [5] X.-W. Li, et al., Progress in selecting desiccant and dehumidifier for liquid desiccant cooling system, *Energy Build.* 49 (2012) 410–418.
- [6] X. Zhao, X. Li, X. Zhang, Selection of optimal mixed liquid desiccants and performance analysis of the liquid desiccant cooling system, *Appl. Therm. Eng.* 94 (2016) 622–634.
- [7] K. Suganthi, K. Rajan, Metal oxide nanofluids: review of formulation, thermo-physical properties, mechanisms, and heat transfer performance, *Renew. Sustain. Energy Rev.* 76 (2017) 226–255.
- [8] N. Shoaib, et al., *Experimental Study of Dehumidification Process by CaCl<sub>2</sub> liquid desiccant containing CuO nanoparticles*, *International Journal of Air-Conditioning and Refrigeration* 28 (1) (2020), 2050009.
- [9] A. Giampieri, et al., An Overview of Solutions for Airborne Viral Transmission Reduction Related to HVAC Systems Including Liquid Desiccant Air-Scrubbing, *Energy*, 2021, 122709.
- [10] A. Brandelli, A.C. Ritter, F.F. Veras, Antimicrobial activities of metal nanoparticles, in: *Metal Nanoparticles in Pharma*, Springer, 2017, pp. 337–363.
- [11] A. Ali, K. Vafai, A.-R. Khaled, Analysis of heat and mass transfer between air and falling film in a cross flow configuration, *Int. J. Heat Mass Tran.* 47 (4) (2004) 743–755.
- [12] A. Ali, K. Vafai, An investigation of heat and mass transfer between air and desiccant film in an inclined parallel and counter flow channels, *Int. J. Heat Mass Tran.* 47 (8–9) (2004) 1745–1760.
- [13] Y.T. Kang, H.J. Kim, K.I. Lee, *Heat and mass transfer enhancement of binary nanofluids for H<sub>2</sub>O/LiBr falling film absorption process*, *Int. J. Refrig.* 31 (5) (2008) 850–856.
- [14] H. Kim, J. Jeong, Y.T. Kang, *Heat and mass transfer enhancement for falling film absorption process by SiO<sub>2</sub> binary nanofluids*, *Int. J. Refrig.* 35 (3) (2012) 645–651.
- [15] L. Omidvar Langroudi, H. Pahlavanzadeh, S. Nanvakenari, *An investigation of heat and mass transfer enhancement of air dehumidification with addition of  $\gamma$ -Al<sub>2</sub>O<sub>3</sub> nano-particles to liquid desiccant*, *Iranian Journal of Chemical Engineering (IJChE)* 13 (4) (2016) 96–112.
- [16] T. Wen, L. Lu, H. Zhong, *Investigation on the dehumidification performance of LiCl/H<sub>2</sub>O-MWNTs nanofluid in a falling film dehumidifier*, *Build. Environ.* 139 (2018) 8–16.
- [17] T. Wen, et al., Experimental and numerical study on the regeneration performance of LiCl solution with surfactant and nanoparticles, *Int. J. Heat Mass Tran.* 127 (2018) 154–164.
- [18] Q. Talal, Modeling and Numerical Investigation of a Falling Film Liquid Desiccant Dehumidifier with Nanoparticles, King Fahd University of Petroleum and Minerals, 2018.
- [19] Y. Zheng, et al., *Experimental investigation of heat and moisture transfer performance of CaCl<sub>2</sub>/H<sub>2</sub>O-SiO<sub>2</sub> nanofluid in a gas–liquid microporous hollow fiber membrane contactor*, *Int. Commun. Heat Mass Tran.* 113 (2020), 104533.
- [20] Y. Lin, F. Xiao, S. Wang, A novel modified LiCl solution for three-phase absorption thermal energy storage and its thermal and physical properties, *Int. J. Refrig.* 130 (2021) 44–55.
- [21] X.-Q. Wang, A.S. Mujumdar, Heat transfer characteristics of nanofluids: a review, *Int. J. Therm. Sci.* 46 (1) (2007) 1–19.
- [22] T. Wen, L. Lu, A review of correlations and enhancement approaches for heat and mass transfer in liquid desiccant dehumidification system, *Appl. Energy* 239 (2019) 757–784.
- [23] T. Wen, L. Lu, C. Dong, Enhancing the dehumidification performance of LiCl solution with surfactant PVP-K30, *Energy Build.* 171 (2018) 183–195.
- [24] T. Wen, et al., Investigation on the regeneration performance of liquid desiccant by adding surfactant PVP-K30, *Int. J. Heat Mass Tran.* 123 (2018) 445–454.
- [25] J. Hu, et al., A dual-scale analysis of mass transfer enhancement in liquid desiccant system for indoor VOCs removal by adding surfactant, *Energy Build.* 273 (2022), 112374.
- [26] Y. Luo, et al., Dehumidification performance of [EMIM] BF<sub>4</sub>, *Appl. Therm. Eng.* 31 (14–15) (2011) 2772–2777.
- [27] Y. Luo, et al., Investigation on feasibility of ionic liquids used in solar liquid desiccant air conditioning system, *Sol. Energy* 86 (9) (2012) 2718–2724.
- [28] M. Qu, et al., Aqueous solution of [EMIM][OAc]: property formulations for use in air conditioning equipment design, *Appl. Therm. Eng.* 124 (2017) 271–278.
- [29] H. Watanabe, et al., Design of ionic liquids as liquid desiccant for an air conditioning system, *Green Energy & Environment* 4 (2) (2019) 139–145.
- [30] T. Turnaoglu, et al., Air Dehumidification Using Ionic Liquid-Based Fiber Bundle Membrane Contactor, 2021.
- [31] S. Maekawa, et al., Design of quaternary ammonium type-ionic liquids as desiccants for an air-conditioning system, *Green Chemical Engineering* 1 (2) (2020) 109–116.
- [32] L. Wang, et al., An experimental study on dehumidification and regeneration performance of a new nonporous membrane-based heat and mass exchanger using an ionic liquid desiccant, *Energy Build.* 254 (2022), 111592.
- [33] M. Sultan, et al., Steady-state investigation of water vapor adsorption for thermally driven adsorption based greenhouse air-conditioning system, *Renew. Energy* 86 (2016) 785–795.
- [34] M. Sultan, T. Miyazaki, S. Koyama, Optimization of adsorption isotherm types for desiccant air-conditioning applications, *Renew. Energy* 121 (2018) 441–450.
- [35] Lithium chloride technical [cited 2022 29 November]; Available from: <https://www.levertonlithium.com/products/lithium-chloride/lithium-chloride-technical/>.
- [36] Tetra calcium chloride flakes [cited 2022 28 November]; Available from: <https://hcsunners.com/catalog/product/130570/tetra-calcium-chloride-flakes-nbsp>.
- [37] Potassium formate, 99% (water less than 2%), Thermo Scientific™. [cited 2022 28 November]; Available from: <https://www.fishersci.co.uk/shop/products/potassium-formate-99-water-less-than-2-thermo-scientific/11411938>.
- [38] Polyvinylpyrrolidone, average M.W. 50.000, K30, thermo Scientific™ [cited 2022 29 November]; Available from: <https://www.thermofisher.com/order/catalog/product/227541000>.
- [39] Copper(II) oxide. [cited 2022 29 November]; Available from: <https://www.sigmaaldrich.com/GB/en/product/aldrich/544868>.
- [40] G. Ren, et al., Characterisation of copper oxide nanoparticles for antimicrobial applications, *Int. J. Antimicrob. Agents* 33 (6) (2009) 587–590.
- [41] P. Wasserscheid, M. Seiler, Leveraging gigawatt potentials by smart heat-pump technologies using ionic liquids, *ChemSusChem* 4 (4) (2011) 459–463.
- [42] S. Fendt, et al., Viscosities of acetate or chloride-based ionic liquids and some of their mixtures with water or other common solvents, *J. Chem. Eng. Data* 56 (1) (2011) 31–34.
- [43] T. Brunig, M. Maurer, R. Pietschnig, Sorbent properties of halide-free ionic liquids for water and CO<sub>2</sub> perfusion, *ACS Sustain. Chem. Eng.* 5 (8) (2017) 7228–7239.
- [44] Ionic Liquid Production. [cited 2022 29 November]; Available from: <https://proionic.com/ionic-liquids/services-ionic-liquid-production.php>.

- [45] C.S. Queiros, et al., [C2mim][CH<sub>3</sub>SO<sub>3</sub>]- A suitable new heat transfer fluid? Part 2: thermophysical properties of its mixtures with water, *Ind. Eng. Chem. Res.* 61 (5) (2022) 2280–2305.
- [46] Kambic KK-105 CH User Manual.
- [47] Lithium chloride price [cited 2023 10 January]; Available from: <https://www.alibaba.com/showroom/lithium-chloride.html>.
- [48] Calcium Chloride price. [cited 2023 10 January]; Available from: <https://www.alibaba.com/showroom/cacl2.html>.
- [49] Potassium Formate price. [cited 2023 10 January]; Available from: <https://www.alibaba.com/showroom/potassium-formate-price.html>.
- [50] Polyvinylpyrrolidone PVP-K30 price. [cited 2023 10 January]; Available from: <https://www.alibaba.com/showroom/polyvinylpyrrolidone-pvp-k30.html>.
- [51] Copper Oxide nanoparticles price [cited 2023 10 January]; Available from: <https://www.alibaba.com/showroom/copper-oxide-nanoparticles.html>.
- [52] [EMIM][OAc] price [cited 2023 10 January]; Available from: [https://www.alibaba.com/trade/search?fsb=y&IndexArea=product\\_en&CatId=&tab=all&SearchText=1-ethyl-3-methylimidazolium+acetate](https://www.alibaba.com/trade/search?fsb=y&IndexArea=product_en&CatId=&tab=all&SearchText=1-ethyl-3-methylimidazolium+acetate).
- [53] M.R. Conde, Properties of aqueous solutions of lithium and calcium chlorides: formulations for use in air conditioning equipment design, *Int. J. Therm. Sci.* 43 (4) (2004) 367–382.
- [54] T. Elmer, *A Novel SOFC Tri-generation System for Building Applications*, Springer, 2016.
- [55] G. Lychnos, J.P. Fletcher, P.A. Davies, Properties of seawater bitters with regard to liquid-desiccant cooling, *Desalination* 250 (1) (2010) 172–178.
- [56] TC-08 Thermocouple Data Logger. [cited 2022 08 November].
- [57] S. Bouzenada, et al., Experimental study on dehumidification/regeneration of liquid desiccant: LiBr solution, *Proc. Comput. Sci.* 32 (2014) 673–680.
- [58] W. Kessling, E. Laevemann, C. Kapfhammer, Energy storage for desiccant cooling systems component development, *Sol. Energy* 64 (4–6) (1998) 209–221.
- [59] H. Wu, T.-W. Chung, M.-H. Lai, Effects of Marangoni convection on the mass transfer performance in a packed-bed absorber, *Ind. Eng. Chem. Res.* 40 (3) (2001) 885–891.
- [60] H. Wu, T.-W. Chung, Discussions of effects of surface tension on water vapor absorbed by triethylene glycol solution films, in: *Heat and Mass Transfer-Advances in Modelling and Experimental Study for Industrial Applications*, IntechOpen, 2018.
- [61] A. Giampieri, et al., A techno-economic evaluation of low-grade excess heat recovery and liquid desiccant-based temperature and humidity control in automotive paint shops, *Energy Convers. Manag.* 261 (2022), 115654.
- [62] M. Ahmadi, K.R. Gluesenkamp, S. Bigham, Energy-efficient sorption-based gas clothes dryer systems, *Energy Convers. Manag.* 230 (2021), 113763.
- [63] A. Giampieri, et al., A review of the current automotive manufacturing practice from an energy perspective, *Appl. Energy* 261 (2020), 114074.
- [64] J. Lizana, et al., Advances in thermal energy storage materials and their applications towards zero energy buildings: a critical review, *Appl. Energy* 203 (2017) 219–239.
- [65] B. Guan, et al., Review of Internally Cooled Liquid Desiccant Air Dehumidification: Materials, Components, Systems, and Performances, *Building and Environment*, 2022, 108747.